Materials and Methods

Reagents

Three SDP derivatives, APL,[14,46] AK530, and AK317, are discussed in the present report. The methods for the synthesis and physicochemical profiles of AK530 and AK317 will be described elsewhere. Tritiation of these three CCR5 inhibitors was conducted as previously reported.[14] The structures of these three CCR5 inhibitors are illustrated in Fig. 1.

Cells, viruses, and anti-HIV-1 assay

CHO cells expressing wild-type CCR5 ($CCR5_{WT}$-CHO cells) or mutant CCR5 ($CCR5_{MT}$-CHO cells)[22] were maintained in Ham's F-12 medium (Invitrogen, Carlsbad, CA), supplemented with 10% fetal calf serum (FCS; HyClone, Logan, UT) in the presence of 100 μg/ml zeomycin (Invitrogen). The MAGI cell line[47] was provided by the National Institutes of Health (NIH) AIDS Research and Reference Reagent Program and cultured in Dulbecco's modified Eagle's medium (DMEM) supplemented with 10% FCS, 200 μg/ml G418, and 100 μg/ml hygromycin B. MAGI-CCR5 cells[48] were maintained in DMEM supplemented with 10% FCS, 200 μg/ml G418, 100 μg/ml hygromycin B, and 100 μg/ml zeomycin. 293T cells were cultured in DMEM with 10% FCS. PBM cells were isolated from buffy coats of HIV-1-seronegative individuals and activated with 10 μg/ml PHA prior to use, as previously described.[8] Two wild-type R5-HIV-1 strains were employed for drug susceptibility assays: $HIV\text{-}1_{Ba\text{-}L}$[49] and $HIV\text{-}1_{JRFL}$.[50] Antiviral assays using PHA-PBM (p24 assay) and MAGI assay using MAGI-CCR5 cells were also conducted as previously reported.[8]

Fluorescence-activated cell sorter analysis and mAb displacement assay

$CCR5_{WT}$-CHO cells (2×10^5) were exposed to differing concentrations (1 nM–1 μM) of a CCR5 inhibitor for 30 min, followed by the addition of a fluorescein-isothiocyanate-conjugated anti-CCR5 mAb, 2D7 (BD PharMingen, San Diego, CA), 45523, 45531, or 45549 (R&D Systems, Minneapolis, MN), and further incubated for 30 min at 4 °C. Cells were washed and analyzed on an flow cytometer (FACSCalibur; BD Biosciences, San Jose, CA). Each fluorescent activity in the presence of a drug was compared to that obtained in the absence of inhibitors and shown as percent control.

Saturation binding assay

A panel of mutant CCR5-expressing CHO cells[22] was used for saturation binding assays. The CHO cell lines expressing mutant CCR5 P84H ($CCR5_{P84H}$-CHO cells), C101A, L104D, F109A, T195A, T195P, T195S, and W248A were newly generated and used. The saturation binding assay using tritiated CCR5 inhibitors ([^{3}H]APL, [^{3}H]AK530, and [^{3}H]AK317) and wild-type or mutant CCR5-expressing CHO cells was conducted as previously described.[14] In brief, wild-type or mutant $CCR5^+$ CHO cells (1.5×10^5 cells/well) were plated onto 48-well flat-bottomed culture plates, incubated for 24 h, exposed to various concentrations of each [^{3}H]CCR5 inhibitor, washed thoroughly, and lysed with 0.5 ml of 1 N NaOH, and radioactivity in the lysates was measured. The K_d (dissociation) values of CCR5 inhibitors and the maximal binding values (B_{max} = number of CCR5 per cell) were calculated based on their specific radioactivity using GRAPHPAD PRISM software (Intuitive Software for Science, San Diego, CA).

CCR5 homology model

A homology model of CCR5 was built as follows. The sequence of CCR5 (352 amino acids) was aligned against the sequence of bovine rhodopsin (348 amino acids). The recently determined crystal structure of bovine rhodopsin by Okada *et al.* was used as the template structure [Protein Data Bank (PDB) accession ID 1U19].[27] The alignment was manually adjusted to ensure that the conserved GPCR residues were aligned as follows: in TM1, N55 of bovine rhodopsin was aligned to N48 of CCR5; in TM2, D83 was aligned to D76; in TM3, E134-R135-Y136 was aligned to D125-R126-Y127; in TM4, W161 was aligned to W153; in TM5, P215 was aligned to P206; in TM6, W265-x266-P267-Y268 was aligned to W248-x249-P250-Y251; in TM7, P303 was aligned to P294; in H8, F313 was aligned to F304. Secondary structure prediction assigned the length of each helix, β-sheet, and loop segment. After building the transmembrane helices, the loops connecting the different transmembrane domains were built using the ultraextended sampling protocol in Prime (Prime, version 1.6, 2007; Schrödinger, LLC, New York, NY), which does a more exhaustive sampling of the loop conformations.[51] The side chains were predicted using the rotamer library of Xiang and Honig.[52] The structure was minimized in implicit water with the OPLS2005 force field,[53] as implemented in MacroModel (MacroModel 9.1, 2005; Schrödinger, LLC).

All atom molecular dynamics simulations, without using any nonbonded cutoff distances, were carried out on CCR5. A constant temperature of 300 K and SHAKE constraints for hydrogen bonds were used. The GB/SA continuum solvation model, with water as the solvent, was used.[54] Using a time step of 1 fs, the structures were equilibrated for 100 ps. The simulation was carried out for 4800 ps on a Linux cluster, and structures were monitored at 50-ps intervals.

Structural modeling of the interactions of CCR5 inhibitors with CCR5

After building the initial model of CCR5, the CCR5–inhibitor complex structures were further defined with an iterative optimization of CCR5 and ligand structures in the presence of each other, using software tools from Schrödinger, LLC, as described below. The conformational flexibilities of both CCR5 and CCR5 inhibitors were taken into account. The molecular structures of AK530, AK317, and APL were obtained by minimization using the MMFF94 force field, as implemented in MacroModel. For each minimized inhibitor configuration, a set of low-energy structures was generated by performing a Monte Carlo sampling of their conformations. Thus, obtained structures were used as starting structures for docking calculations where their conformations were further refined.

The protonation states of CCR5 residues were assigned, and residues more than 20 Å from the active site were neutralized. We initially failed to obtain energetically favorable inhibitor–CCR5 complex structures by using a *rigid* CCR5 structure because of the unfavorable steric interaction of the side chains of the active site residues with the inhibitors. In an attempt to place an inhibitor within CCR5, after analysis of the steric clashes, the active site

was artificially enlarged by mutating Y108, C178, E283, and M287 to Ala. The van der Waals radii of inhibitor atoms were scaled by a factor of 0.70 to reduce steric clashes and docked into CCR5. After obtaining an initial "guess" set of CCR5–inhibitor complexes, residues 108, 178, 283, and 287 were mutated back from Ala to their original states. CCR5 atoms within 15 Å of an initially placed inhibitor were subsequently refined. It was achieved by using the rotamer library of Xiang and Honig and by optimizing each side chain one at a time, holding all other side chains fixed.[52] After convergence, all side chains were simultaneously energy-minimized to remove any remaining clashes. The inhibitors were docked again and scored to estimate their relative affinity. The extraprecision mode of Glide,[55,56] which penalized unfavorable and unphysical interactions, was used. The docked complexes with higher scores were visually examined along with the mutational data to select the best possible CCR5–inhibitor complex.

Visualization, structural refinement, and docking were performed using Maestro 7.5, MacroModel 9.1, Prime 1.6, Glide 4.5, and IFD script[38] from Schrödinger, LLC (2007). Computations were carried out on a multiprocessor SGI Origin 3400 computer platform and on a Beowulf-type Linux cluster.

HIV-1-gp120-elicited cell–cell fusion assay

The entire human *CCR5* gene, including a stop codon, was amplified using pZeoSV-*CCR5*[48] as template. The polymerase chain reaction product was ligated into pcDNA6.2/cLumio-DEST vector (Invitrogen), cloned in accordance with the manufacturer's recommendation, and termed pcDNA6.2-CCR5$_{WT}$ (a CCR5 expression vector). A variety of plasmids carrying a mutant *CCR5*-encoding gene (pcDNA6.2-CCR5$_{MT}$) were subsequently generated by employing the site-directed mutagenesis technique. An HIV-1 *tat* expression vector (pcDNA6.2-HIV-*tat*) was also generated using the same method. For the generation of HIV-1-gp120-overexpressing 293T cells, an HIV envelope expression vector, pCXN-J*Renv*,[48] was employed. A reporter (luciferase) gene containing plasmid pLTR-*Luc*E[57] was provided by the NIH AIDS Research and Reference Reagent Program. The envelope expression vector and tat expression vector (0.5 μg each) were cotransfected into 293T cells (2×10^5; 3 ml in six-well microculture plates) using Lipofectamine 2000 (Invitrogen), while the CCR5$_{WT}$ or mutant CCR5 expression vector and pLTR-*Luc*E (0.5 μg each) were cotransfected into MAGI cells (2×10^5; 3 ml in six-well microculture plates). On the next day, both the cotransfected cells were harvested and mixed in a well of 96-well plates (2×10^4 cells each). The cotransfected cells were incubated further for 6 h, the luciferase activity in each well was detected using Bright-Glo Luciferase Assay System (Promega, Madison, WI), and its luminescence level was measured using Veritas Microplate Luminometer (Turner BioSystmes, Sunnyvale, CA). Nonspecific luciferase activity was determined with the luminescence level in the well containing control tat$^+$,*env*$^-$ 293T cells and Luc$^+$,CCR5$^+$ MAGI cells, and the value of the nonspecific luminescence level was subtracted from each experimental luminescence level.

Protein Model DataBase accession code

The coordinates for the models of ligand-free CCR5, CCR5–AK317, and CCR5–AK530 complexes with accession codes PM0075224, PM0075223, and PM0075221, respectively, have been deposited in the Protein Model DataBase†.

Acknowledgements

The authors thank David A. Davis and Yasuhiro Koh for critical reading of the manuscript. This work was supported, in part, by the Intramural Research Program of the Center for Cancer Research, National Cancer Institute, NIH, and in part by a Grant for the Promotion of AIDS Research from the Ministry of Health, Welfare, and Labor of Japan, and the Grant to the Cooperative Research Project on Clinical and Epidemiological Studies of Emerging and Reemerging Infectious Diseases (Renkei Jigyo: No. 78, Kumamoto University) of Monbu-Kagakusho (H. M.). We also thank the Center for Information Technology, NIH, for providing computational resources on the NIH Beowulf Linux cluster, and Susan Chacko and David Hoover for help with batch job configuration on the cluster.

References

1. Raport, C. J., Gosling, J., Schweickart, V. L., Gray, P. W. & Charo, I. F. (1996). Molecular cloning and functional characterization of a novel human CC chemokine receptor (CCR5) for RANTES, MIP-1beta, and MIP-1alpha. *J. Biol. Chem.* **271**, 17161–17166.
2. Alkhatib, G., Combadiere, C., Broder, C. C., Feng, Y., Kennedy, P. E., Murphy, P. M. & Berger, E. A. (1996). CC CKR5: a RANTES, MIP-1alpha, MIP-1beta receptor as a fusion cofactor for macrophage-tropic HIV-1. *Science*, **272**, 1955–1958.
3. Wu, L., Gerard, N. P., Wyatt, R., Choe, H., Parolin, C., Ruffing, N. *et al.* (1996). CD4-induced interaction of primary HIV-1 gp120 glycoproteins with the chemokine receptor CCR-5. *Nature*, **384**, 179–183.
4. Trkola, A., Dragic, T., Arthos, J., Binley, J. M., Olson, W. C., Allaway, G. P. *et al.* (1996). CD4-dependent, antibody-sensitive interactions between HIV-1 and its co-receptor CCR-5. *Nature*, **384**, 184–187.
5. Deng, H., Liu, R., Ellmeier, W., Choe, S., Unutmaz, D., Burkhart, M. *et al.* (1996). Identification of a major co-receptor for primary isolates of HIV-1. *Nature*, **381**, 661–666.
6. Kilby, J. M. & Eron, J. J. (2003). Novel therapies based on mechanisms of HIV-1 cell entry. *N. Engl. J. Med.* **348**, 2228–2238.
7. Baba, M., Nishimura, O., Kanzaki, N., Okamoto, M., Sawada, H., Iizawa, Y. *et al.* (1999). A small-molecule, nonpeptide CCR5 antagonist with highly potent and selective anti-HIV-1 activity. *Proc. Natl Acad. Sci. USA*, **96**, 5698–5703.
8. Maeda, K., Yoshimura, K., Shibayama, S., Habashita, H., Tada, H., Sagawa, K. *et al.* (2001). Novel low molecular weight spirodiketopiperazine derivatives potently inhibit R5 HIV-1 infection through their antagonistic effects on CCR5. *J. Biol. Chem.* **276**, 35194–35200.

† http://mi.caspur.it/PMDB

9. Watson, C., Jenkinson, S., Kazmierski, W. & Kenakin, T. (2005). The CCR5 receptor-based mechanism of action of 873140, a potent allosteric noncompetitive HIV entry inhibitor. *Mol. Pharmacol.* **67**, 1268–1282.
10. Tagat, J. R., McCombie, S. W., Nazareno, D., Labroli, M. A., Xiao, Y., Steensma, R. W. *et al.* (2004). Piperazine-based CCR5 antagonists as HIV-1 inhibitors: IV. Discovery of 1-[(4,6-dimethyl-5-pyrimidinyl)carbonyl]-4-[4-[2-methoxy-1(*R*)-4-(trifluoromethyl)phenyl] ethyl-3(*S*)-methyl-1-piperaz inyl]-4-methylpiperidine (Sch-417690/Sch-D), a potent, highly selective, and orally bioavailable CCR5 antagonist. *J. Med. Chem.* **47**, 2405–2408.
11. Dorr, P., Westby, M., Dobbs, S., Griffin, P., Irvine, B., Macartney, M. *et al.* (2005). Maraviroc (UK-427,857), a potent, orally bioavailable, and selective small-molecule inhibitor of chemokine receptor CCR5 with broad-spectrum anti-human immunodeficiency virus type 1 activity. *Antimicrob. Agents Chemother.* **49**, 4721–4732.
12. Seto, M., Aikawa, K., Miyamoto, N., Aramaki, Y., Kanzaki, N., Takashima, K. *et al.* (2006). Highly potent and orally active CCR5 antagonists as anti-HIV-1 agents: synthesis and biological activities of 1-benzazocine derivatives containing a sulfoxide moiety. *J. Med. Chem.* **49**, 2037–2048.
13. Imamura, S., Ichikawa, T., Nishikawa, Y., Kanzaki, N., Takashima, K., Niwa, S. *et al.* (2006). Discovery of a piperidine-4-carboxamide CCR5 antagonist (TAK-220) with highly potent anti-HIV-1 activity. *J. Med. Chem.* **49**, 2784–2793.
14. Maeda, K., Nakata, H., Koh, Y., Miyakawa, T., Ogata, H., Takaoka, Y. *et al.* (2004). Spirodiketopiperazine-based CCR5 inhibitor which preserves CC-chemokine/CCR5 interactions and exerts potent activity against R5 human immunodeficiency virus type 1 *in vitro*. *J. Virol.* **78**, 8654–8662.
15. Fatkenheuer, G., Pozniak, A. L., Johnson, M. A., Plettenberg, A., Staszewski, S., Hoepelman, A. I. *et al.* (2005). Efficacy of short-term monotherapy with maraviroc, a new CCR5 antagonist, in patients infected with HIV-1. *Nat. Med.* **11**, 1170–1172.
16. Cormier, E. G. & Dragic, T. (2002). The crown and stem of the V3 loop play distinct roles in human immunodeficiency virus type 1 envelope glycoprotein interactions with the CCR5 coreceptor. *J. Virol.* **76**, 8953–8957.
17. Huang, C. C., Tang, M., Zhang, M. Y., Majeed, S., Montabana, E., Stanfield, R. L. *et al.* (2005). Structure of a V3-containing HIV-1 gp120 core. *Science*, **310**, 1025–1028.
18. Kondru, R., Zhang, J., Ji, C., Mirzadegan, T., Rotstein, D., Sankuratri, S. & Dioszegi, M. (2008). Molecular interactions of CCR5 with major classes of small-molecule anti-HIV CCR5 antagonists. *Mol. Pharmacol.* **73**, 789–800.
19. Dragic, T., Trkola, A., Thompson, D. A., Cormier, E. G., Kajumo, F. A., Maxwell, E. *et al.* (2000). A binding pocket for a small molecule inhibitor of HIV-1 entry within the transmembrane helices of CCR5. *Proc. Natl Acad. Sci. USA*, **97**, 5639–5644.
20. Nishikawa, M., Takashima, K., Nishi, T., Furuta, R. A., Kanzaki, N., Yamamoto, Y. & Fujisawa, J. (2005). Analysis of binding sites for the new small-molecule CCR5 antagonist TAK-220 on human CCR5. *Antimicrob. Agents Chemother.* **49**, 4708–4715.
21. Seibert, C., Ying, W., Gavrilov, S., Tsamis, F., Kuhmann, S. E., Palani, A. *et al.* (2006). Interaction of small molecule inhibitors of HIV-1 entry with CCR5. *Virology*, **349**, 41–54.
22. Maeda, K., Das, D., Ogata-Aoki, H., Nakata, H., Miyakawa, T., Tojo, Y. *et al.* (2006). Structural and molecular interactions of CCR5 inhibitors with CCR5. *J. Biol. Chem.* **281**, 12688–12698.
23. Tsamis, F., Gavrilov, S., Kajumo, F., Seibert, C., Kuhmann, S., Ketas, T. *et al.* (2003). Analysis of the mechanism by which the small-molecule CCR5 antagonists SCH-351125 and SCH-350581 inhibit human immunodeficiency virus type 1 entry. *J. Virol.* **77**, 5201–5208.
24. Nakata, H., Maeda, K., Miyakawa, T., Shibayama, S., Matsuo, M., Takaoka, Y. *et al.* (2005). Potent anti-R5 human immunodeficiency virus type 1 effects of a CCR5 antagonist, AK602/ONO4128/GW873140, in a novel human peripheral blood mononuclear cell nonobese diabetic-SCID, interleukin-2 receptor gamma-chain-knocked-out AIDS mouse model. *J. Virol.* **79**, 2087–2096.
25. Wu, L., LaRosa, G., Kassam, N., Gordon, C. J., Heath, H., Ruffing, N. *et al.* (1997). Interaction of chemokine receptor CCR5 with its ligands: multiple domains for HIV-1 gp120 binding and a single domain for chemokine binding. *J. Exp. Med.* **186**, 1373–1381.
26. Samson, M., LaRosa, G., Libert, F., Paindavoine, P., Detheux, M., Vassart, G. & Parmentier, M. (1997). The second extracellular loop of CCR5 is the major determinant of ligand specificity. *J. Biol. Chem.* **272**, 24934–24941.
27. Okada, T., Sugihara, M., Bondar, A. N., Elstner, M., Entel, P. & Buss, V. (2004). The retinal conformation and its environment in rhodopsin in light of a new 2.2 A crystal structure. *J. Mol. Biol.* **342**, 571–583.
28. Gether, U. & Kobilka, B. K. (1998). G protein-coupled receptors: II. Mechanism of agonist activation. *J. Biol. Chem.* **273**, 17979–17982.
29. Farrens, D. L., Altenbach, C., Yang, K., Hubbell, W. L. & Khorana, H. G. (1996). Requirement of rigid-body motion of transmembrane helices for light activation of rhodopsin. *Science*, **274**, 768–770.
30. Okada, T., Fujiyoshi, Y., Silow, M., Navarro, J., Landau, E. M. & Shichida, Y. (2002). Functional role of internal water molecules in rhodopsin revealed by X-ray crystallography. *Proc. Natl Acad. Sci. USA*, **99**, 5982–5987.
31. Siciliano, S. J., Kuhmann, S. E., Weng, Y., Madani, N., Springer, M. S., Lineberger, J. E. *et al.* (1999). A critical site in the core of the CCR5 chemokine receptor required for binding and infectivity of human immunodeficiency virus type 1. *J. Biol. Chem.* **274**, 1905–1913.
32. Palczewski, K., Kumasaka, T., Hori, T., Behnke, C. A., Motoshima, H., Fox, B. A. *et al.* (2000). Crystal structure of rhodopsin: a G protein-coupled receptor. *Science*, **289**, 739–745.
33. Rosenkilde, M. M. & Schwartz, T. W. (2006). GluVII:06—a highly conserved and selective anchor point for non-peptide ligands in chemokine receptors. *Curr. Top. Med. Chem.* **6**, 1319–1333.
34. Ballesteros, J. A., Jensen, A. D., Liapakis, G., Rasmussen, S. G., Shi, L., Gether, U. & Javitch, J. A. (2001). Activation of the beta 2-adrenergic receptor involves disruption of an ionic lock between the cytoplasmic ends of transmembrane segments 3 and 6. *J. Biol. Chem.* **276**, 29171–29177.
35. Olson, W. C., Rabut, G. E., Nagashima, K. A., Tran, D. N., Anselma, D. J., Monard, S. P. *et al.* (1999). Differential inhibition of human immunodeficiency virus type 1 fusion, gp120 binding, and CC-chemokine activity by monoclonal antibodies to CCR5. *J. Virol.* **73**, 4145–4155.
36. Lee, B., Sharron, M., Blanpain, C., Doranz, B. J., Vakili, J., Setoh, P. *et al.* (1999). Epitope mapping of CCR5 reveals multiple conformational states and distinct but overlapping structures involved in chemokine and coreceptor function. *J. Biol. Chem.* **274**, 9617–9626.

37. Rasmussen, S. G., Choi, H. J., Rosenbaum, D. M., Kobilka, T. S., Thian, F. S., Edwards, P. C. *et al.* (2007). Crystal structure of the human beta$_2$ adrenergic G-protein-coupled receptor. *Nature*, **450**, 383–387.
38. Sherman, W., Day, T., Jacobson, M. P., Friesner, R. A. & Farid, R. (2006). Novel procedure for modeling ligand/receptor induced fit effects. *J. Med. Chem.* **49**, 534–553.
39. Kuhmann, S. E., Pugach, P., Kunstman, K. J., Taylor, J., Stanfield, R. L., Snyder, A. *et al.* (2004). Genetic and phenotypic analyses of human immunodeficiency virus type 1 escape from a small-molecule CCR5 inhibitor. *J. Virol.* **78**, 2790–2807.
40. Trkola, A., Kuhmann, S. E., Strizki, J. M., Maxwell, E., Ketas, T., Morgan, T. *et al.* (2002). HIV-1 escape from a small molecule, CCR5-specific entry inhibitor does not involve CXCR4 use. *Proc. Natl Acad. Sci. USA*, **99**, 395–400.
41. Baba, M., Miyake, H., Wang, X., Okamoto, M. & Takashima, K. (2007). Isolation and characterization of human immunodeficiency virus type 1 resistant to the small-molecule CCR5 antagonist TAK-652. *Antimicrob. Agents Chemother.* **51**, 707–715.
42. Westby, M., Smith-Burchnell, C., Mori, J., Lewis, M., Mosley, M., Stockdale, M. *et al.* (2007). Reduced maximal inhibition in phenotypic susceptibility assays indicates that viral strains resistant to the CCR5 antagonist maraviroc utilize inhibitor-bound receptor for entry. *J. Virol.* **81**, 2359–2371.
43. Marozsan, A. J., Kuhmann, S. E., Morgan, T., Herrera, C., Rivera-Troche, E., Xu, S. *et al.* (2005). Generation and properties of a human immunodeficiency virus type 1 isolate resistant to the small molecule CCR5 inhibitor, SCH-417690 (SCH-D). *Virology*, **338**, 182–199.
44. Pugach, P., Marozsan, A. J., Ketas, T. J., Landes, E. L., Moore, J. P. & Kuhmann, S. E. (2007). HIV-1 clones resistant to a small molecule CCR5 inhibitor use the inhibitor-bound form of CCR5 for entry. *Virology*, **361**, 212–228.
45. LaBranche, C., Kitrinos, K., Howell, R., McDanal, C., Harris, S., Jeffrey, J. & Demarest, J. (2005). Targeting HIV Entry, 1st International Workshop, Bethesda, MD, December 2–3, Abstract 9.
46. Nishizawa, R., Nishiyama, T., Hisaichi, K., Matsunaga, N., Minamoto, C., Habashita, H. *et al.* (2007). Spirodiketopiperazine-based CCR5 antagonists: lead optimization from biologically active metabolite. *Bioorg. Med. Chem. Lett.* **17**, 727–731.
47. Kimpton, J. & Emerman, M. (1992). Detection of replication-competent and pseudotyped human immunodeficiency virus with a sensitive cell line on the basis of activation of an integrated beta-galactosidase gene. *J. Virol.* **66**, 2232–2239.
48. Maeda, Y., Foda, M., Matsushita, S. & Harada, S. (2000). Involvement of both the V2 and V3 regions of the CCR5-tropic human immunodeficiency virus type 1 envelope in reduced sensitivity to macrophage inflammatory protein 1alpha. *J. Virol.* **74**, 1787–1793.
49. Gartner, S., Markovits, P., Markovitz, D. M., Kaplan, M. H., Gallo, R. C. & Popovic, M. (1986). The role of mononuclear phagocytes in HTLV-III/LAV infection. *Science*, **233**, 215–219.
50. Koyanagi, Y., O'Brien, W. A., Zhao, J. Q., Golde, D. W., Gasson, J. C. & Chen, I. S. (1988). Cytokines alter production of HIV-1 from primary mononuclear phagocytes. *Science*, **241**, 1673–1675.
51. Jacobson, M. P., Pincus, D. L., Rapp, C. S., Day, T. J., Honig, B., Shaw, D. E. & Friesner, R. A. (2004). A hierarchical approach to all-atom protein loop prediction. *Proteins*, **55**, 351–367.
52. Xiang, Z. & Honig, B. (2001). Extending the accuracy limits of prediction for side-chain conformations. *J. Mol. Biol.* **311**, 421–430.
53. Kaminski, G. A., Friesner, R. A., Tirado-Rives, J. & Jorgensen, W. J. (2001). Evaluation and reparameterization of the OPLS-AA force field for proteins via comparison with accurate quantum chemical calculations on peptides. *J. Phys. Chem. B*, **105**, 6474–6487.
54. Still, W. C., Tempczyk, A., Hawley, R. C. & Hendrickson, T. (1990). Semianalytical treatment of solvation for molecular mechanics and dynamics. *J. Am. Chem. Soc.* **112**, 6127–6129.
55. Friesner, R. A., Banks, J. L., Murphy, R. B., Halgren, T. A., Klicic, J. J., Mainz, D. T. *et al.* (2004). Glide: a new approach for rapid, accurate docking and scoring: 1. Method and assessment of docking accuracy. *J. Med. Chem.* **47**, 1739–1749.
56. Friesner, R. A., Murphy, R. B., Repasky, M. P., Frye, L. L., Greenwood, J. R., Halgren, T. A. *et al.* (2006). Extra precision Glide: docking and scoring incorporating a model of hydrophobic enclosure for protein–ligand complexes. *J. Med. Chem.* **49**, 6177–6196.
57. Jeeninga, R. E., Hoogenkamp, M., Armand-Ugon, M., de Baar, M., Verhoef, K. & Berkhout, B. (2000). Functional differences between the long terminal repeat transcriptional promoters of human immunodeficiency virus type 1 subtypes A through G. *J. Virol.* **74**, 3740–3751.

The International Journal of Biochemistry & Cell Biology 40 (2008) 2410–2420

Contents lists available at ScienceDirect

The International Journal of Biochemistry & Cell Biology

journal homepage: www.elsevier.com/locate/biocel

2′-Deoxy-4′-*C*-ethynyl-2-halo-adenosines active against drug-resistant human immunodeficiency virus type 1 variants

Atsushi Kawamoto[a], Eiichi Kodama[a,*], Stefan G. Sarafianos[b], Yasuko Sakagami[a], Satoru Kohgo[c], Kenji Kitano[c], Noriyuki Ashida[c], Yuko Iwai[c], Hiroyuki Hayakawa[c], Hirotomo Nakata[d,e], Hiroaki Mitsuya[d,e], Eddy Arnold[f], Masao Matsuoka[a]

[a] *Laboratory of Virus Immunology, Institute for Virus Research, Kyoto University, 53 Kawaramachi, Shogoin, Sakyo-ku, Kyoto 606-8507, Japan*
[b] *Department of Molecular Microbiology and Immunology, University of Missouri-Columbia, School of Medicine and Christopher S. Bond Life Sciences Center, Columbia, MO 65211, USA*
[c] *Biochemicals Division, Yamasa Corporation, Chiba 288-0056, Japan*
[d] *Department of Hematology and Infectious Diseases, Kumamoto University School of Medicine, Kumamoto 860-8556, Japan*
[e] *Experimental Retrovirology Section, HIV and AIDS Malignancy Branch, National Cancer Institute, Bethesda, MD 20892, USA*
[f] *Center for Advanced Biotechnology and Medicine and Department of Chemistry and Chemical Biology, Rutgers University, Piscataway, NJ 08854, USA*

ARTICLE INFO

Article history:
Received 3 December 2007
Received in revised form 14 March 2008
Accepted 2 April 2008
Available online 11 April 2008

Keywords:
Human immunodeficiency virus
Reverse transcriptase inhibitor
Resistance

ABSTRACT

One of the formidable challenges in therapy of infections by human immunodeficiency virus (HIV) is the emergence of drug-resistant variants that attenuate the efficacy of highly active antiretroviral therapy (HAART). We have recently introduced 4′-ethynyl-nucleoside analogs as nucleoside reverse transcriptase inhibitors (NRTIs) that could be developed as therapeutics for treatment of HIV infections. In this study, we present 2′-deoxy-4′-*C*-ethynyl-2-fluoroadenosine (EFdA), a second generation 4′-ethynyl inhibitor that exerted highly potent activity against wild-type HIV-1 ($EC_{50} \sim 0.07$ nM). EFdA retains potency toward many HIV-1 resistant strains, including the multi-drug resistant clone HIV-$1_{A62V/V75I/F77L/F116Y/Q151M}$. The selectivity index of EFdA (cytotoxicity/inhibitory activity) is more favorable than all approved NRTIs used in HIV therapy. Furthermore, EFdA efficiently inhibited clinical isolates from patients heavily treated with multiple anti-HIV-1 drugs. EFdA appears to be primarily phosphorylated by the cellular 2′-deoxycytidine kinase (dCK) because: (a) the antiviral activity of EFdA was reduced by the addition of dC, which competes nucleosides phosphorylated by the dCK pathway, (b) the antiviral activity of EFdA was significantly reduced in dCK-deficient HT-1080/Ara-C^r cells, but restored after dCK transduction. Further, unlike other dA analogs, EFdA is completely resistant to degradation by adenosine deaminase. Moderate decrease in susceptibility to EFdA is conferred by a combination of three RT mutations (I142V, T165R, and M184V) that result in a significant decrease of viral fitness. Molecular modeling analysis suggests that the M184V/I substitutions may reduce anti-HIV activity of EFdA through steric hindrance between its 4′-ethynyl moiety and the V/I184 β-branched side chains. The present data suggest that EFdA, is a promising candidate for developing as a therapeutic agent for the treatment of individuals harboring multi-drug resistant HIV variants.

1. Introduction

Highly active antiretroviral therapies (HAART), combining two or more reverse transcriptase inhibitors (RTIs) and/or protease inhibitors, have been successful in sig-

* Corresponding author. Tel.: +81 75 751 3986; fax: +81 75 751 3986.
E-mail address: ekodama@virus.kyoto-u.ac.jp (E. Kodama).

1357-2725/$ – see front matter © 2008 Elsevier Ltd. All rights reserved.
doi:10.1016/j.biocel.2008.04.007

nificantly reducing viral loads and bringing about clinical benefits to the treatment of patients infected with human immunodeficiency virus type 1 (HIV-1). Although HAART improves prognosis for HIV-1 infected patients (Palella et al., 1998), drug-resistant viruses emerge during prolonged therapy and some resistant viruses show intra-class cross resistance. Moreover, drug-resistant variants can be transmitted to other individuals as primary infections (Little et al., 2002). Hence, there is a great need for the development of new HIV inhibitors that retain activity against drug-resistant HIV variants.

In this regard, we have focused on the family of nucleoside reverse transcriptase inhibitors (NRTIs) and have previously reported that a series of 2′-deoxy-4′-C-ethynyl-nucleosides (EdNs) efficiently suppress (EC_{50}s as low as one nanomolar) various NRTI-resistant HIV strains including multi-drug resistant clinical isolates (Kodama et al., 2001). More recently, Haraguchi and others have reported that additional members of EdNs such as 2′,3′-didehydro-3′-deoxy-4′-C-ethynyl-thymidine (Ed4T) are also active against wild-type and drug-resistant strains (EC_{50}s ranged from 0.16 to 17 μM) and less toxic than d4T (also known as stavudine) *in vitro* (Dutschman et al., 2004; Haraguchi et al., 2003), while 4′-Ed4T is only moderately active against (−)-2′,3′-dideoxy-3′-thiacytidine (3TC or lamivudine)-resistant HIV-1_{M184V} (Nitanda et al., 2005).

To further increase the antiviral activity and reduce the cytotoxicity, we designed and synthesized a second generation of 4′-substituted adenosine analogs with halogen substitutions at their 2-position. We report here that 2′-deoxy-4′-C-ethynyl-2-fluoroadenosine (EFdA) exhibits the highest antiviral activity than any other NRTI when assayed against wild-type or NRTI-resistant HIV clones and clinical isolates from patients treated extensively with anti-HIV agents. In addition, unlike other adenosine-based NRTIs, EFdA showed adenosine deaminase (ADA) resistance. We also show that EFdA is primarily activated through phosphorylation by cellular deoxycytidine kinase (dCK). Molecular modeling analysis has been used to rationalize the resistance profile of these analogs toward key NRTI mutations.

2. Materials and methods

2.1. Compounds

3′-Azido-3′-deoxythymidine (AZT, or zidovudine), 2′,3′-dideoxyinosine (ddI, or didanosine), and 2′,3′-dideoxycytidine (ddC, or zalcitabine) were purchased from Sigma (St. Louis, MO.). 3TC was kindly provided from S. Shigeta (Fukushima Medical University, Fukushima, Japan). A set of EdN analogs were designed and synthesized as described elsewhere (Ohrui, 2006). Their chemical structures are shown in Fig. 1. 2′-Deoxycoformycin (dCF) was synthesized in Yamasa Corporation (Choshi, Japan).

2.2. Cells and plasmids

MT-2 and MT-4 cells were grown in an RPMI 1640-based culture medium, and 293T cells were grown in Dulbecco's modified Eagle medium (DMEM); each of these media was supplemented with 10% fetal calf serum (FCS), 2 mM L-glutamine, 100 U/ml penicillin, and 50 μg/ml streptomycin. HeLa-CD4-LTR/β-galactosidase (MAGI) cells were propagated in DMEM supplemented with 10% FCS, 0.2 mg/ml of hygromycin B, and 0.2 mg/ml of G418 (Kimpton and Emerman, 1992). HeLa-CD4/CCR5-LTR/β-galactosidase cells were propagated in puromycin (10 μg/ml) containing DMEM with hygromycin and G418. Peripheral blood mononuclear cells (PBMCs) were obtained from healthy HIV-1-seronegative donors by Ficoll-Hypaque gradient centrifugation and stimulated for 3 days with phytohemagglutinin M (PHA; 10 μg/ml; Sigma) and recombinant human interleukin 2 (IL-2; 10 U/ml; Shionogi & Co., Ltd., Osaka, Japan) prior to use. Human fibrosarcoma cell lines, HT-1080 and HT-1080/Ara-C^r were grown in the RPMI-based culture medium (Obata et al., 2001). To express HIV-1 receptors, we constructed a mammalian expression vector pBC-CD4/CXCR4-IH, which encodes CD4, CXCR4, and hygromycin phosphotransferase with two internal ribosome entry sites under control of cytomegalovirus promoter as described (Kajiwara et al., 2006). After the transfection into HT-1080 and HT-1080/Ara-C^r, cells were selected by 0.2 mg/ml hygromycin B. For the expression of human deoxycytidine kinase (dCK), pCI-neo (Promega, Madison, WI)-based plasmid, pCI-dCK, was transfected into HT-1080/Ara-C^r and selected with 0.2 mg/ml G418. Established cells were designated HT-1080/Ara-C^r/dCK. Puromycin resistance gene under the control of PGK promoter was inserted into pLTR-SEAP (Miyake et al., 2003), which encodes a secreted form of the placental alkaline phosphatase (SEAP) gene under control of the HIV-1 long terminal repeat (LTR) (pLTR-SEAP-puro^r). pLTR-SEAP-puro^r was transfected into the three HT-1080 cell lines and selected with 10 μg/ml puromycin.

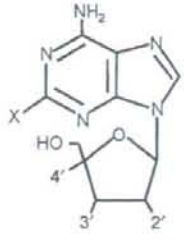

Base X	Sugar 2′	Sugar 3′	4′	Compound abbreviation
-H	-H	-OH	-C ≡ CH	*E*dA
-F	-H	-OH	-C ≡ CH	2F-*E*dA
-F	-H	-H	-C ≡ CH	2F-*E*ddA
-F	C = C		-C ≡ CH	2F-*E*d4A
-F	-H	-OH	-C ≡ N	2F-CNdA
-Cl	-H	-OH	-C ≡ CH	2Cl-*E*dA

Fig. 1. Structures of 4′-substituted adenosine analogs. All nucleoside analogs discussed here have substitutions at the 4′-position of the sugar ring.

2.3. Viruses and construction of recombinant HIV-1 clones

Two laboratory strains, HIV-1_{IIIB} and HIV-2_{EHO}, were used. Multi-drug resistant clinical HIV-1 strains, which had been exposed to over 10 anti-HIV-1 drugs for at least 3 years, were passaged in PHA-stimulated PBMCs (PHA-PBMCs) and stored at −80 °C until further use. Recombinant infectious HIV-1 clones carrying various mutations in the *pol* gene were generated using pNL101 (Jeang et al., 1993). Briefly, desired mutations were introduced into the XmaI–NheI region (759 bp) of pTZNX1, which encoded Gly-15 to Ala-267 of HIV-1 RT (strain BH 10) by a site-directed mutagenesis method (Weiner et al., 1994). The XmaI–NheI fragment was inserted into a pNL101-based plasmid, pNL-RT, generating various molecular clones with the desired mutations. To generate pNL-RT, we first introduced a silent mutation at NheI site of the pNL101, GCTAGC to GCCAGC (underlined; 7251 n.t. from the 5′-LTR) by site-directed mutagenesis. Then, the ApaI–SalI fragment of pNL101 without the NheI site was replaced with that of pSUM9 (Shirasaka et al., 1995), to introduce XmaI and NheI site in the RT coding region. The presence of intended substitutions and the absence of unintended substitutions in the molecular clones were confirmed by sequencing. Each molecular clone (2 μg/ml as DNA) was transfected into 293T cells (4×10^5 cells/6-well plate) by FuGENE 6 Transfection Reagent (Roche Diagnostics, Indianapolis, IN). After 24 h, MT-2 cells (10^6 cells/well) were added and co-cultured with 293T cells for an additional 24 h. When an extensive cytopathic effect was observed, the cell supernatants were harvested, and the virus was further propagated in MT-4 cells. The culture supernatant was harvested and stored at −80 °C until further use.

2.4. Determination of drug susceptibility

The inhibitory effect of test compounds on viral replication for 5 days was evaluated in MT-4 cells by the MTT method as described previously (Kodama et al., 2001). The sensitivity of NRTI-resistant infectious clones to test compounds was determined by the MAGI assay as described (Nameki et al., 2005). The drug susceptibility of HIV-1 clinical isolates was determined on day 7 by a commercially available p24 antigen assay (Kodama et al., 2001). Briefly, PHA-PBMCs (10^6 cells/ml) were exposed to each viral preparation at $TCID_{50}$ of 50 and cultivated in 200 μl of culture medium containing various concentration of the drug in 96-well culture plates. All assays were performed in triplicate, and the amounts of p24 antigen produced by the cells into the culture medium were determined. A 2′-deoxynucleoside competition assay was performed by the same way as the MAGI assay. An adenosine deaminase (ADA) inhibitor, dCF, was added for preventing conversion of 2′-deoxyadenosine (dA) to 2′-deoxyinosine (dI) (final concentration 0.4 μM). The effect of dCK expression on activities of test compounds was examined by measurement of SEAP activity in the supernatant. At first, the target cells (HT-1080, HT-1080/Ara-C^r, and HT-1080/Ara-C^r/dCK) were suspended in 96-well plates (5.0×10^3 cells/well). On the following day, the cells were inoculated with HIV-1_{IIIB} (500 MAGI unit/well, giving 500 blue cells in MAGI cells) in the presence of serially diluted compounds. After 48 h incubation, supernatant was collected and SEAP activity in the supernatant was measured using BD Great EscAPe SEAP chemiluminescence detection kit (BD Biosciences Clontech., Palo Alto, CA) and Wallac 1450 MicroBeta Jet Luminometer (PerkinElmer, Wellesley, MA).

2.5. The effect of ADA

The effect of ADA on EdA or EFdA was examined by high performance liquid chromatography (HPLC). ADA (0.01 U) derived from bovine intestinal tract was added into 0.5 ml of 0.5 mM EFdA in 50 mM Tris–HCl buffer (pH 7.5), and incubated at 25 °C. Samples were collected each 15 min and analyzed by HPLC.

2.6. HIV-1 replication assays

MT-2 cells (2.5×10^5 cells/5 ml) were infected with each virus preparation (500 MAGI units) for 4 h. The infected cells were then washed and cultured in a final volume of 5 ml. Culture supernatants (200 μl) were harvested from days 1 to 7 after infection, and the p24 antigen amounts were quantified (Nameki et al., 2005).

For competitive HIV-1 replication assay (CHRA), two titrated infectious clones to be examined were mixed and added to MT-2 cells (10^5 cells/3 ml) as described previously (Kosalaraksa et al., 1999; Nameki et al., 2005). To ensure that the two infectious clones being compared were of approximately equal infectivity, a fixed amount (500 MAGI units) of one infectious clone was mixed with three different amounts (250, 500 and 1000 MAGI units) of the other infectious clone. On day 1, one-third of the infected MT-2 cells were harvested, washed twice with phosphate-buffered saline, and the cellular DNA was extracted. The purified DNA was subjected to nested PCR and then direct DNA sequencing. The HIV-1 coculture which best approximated a 50:50 mixture on day 1 was further propagated. Every 4–6 days, the cell-free supernatant of the virus coculture (1 ml) was transmitted to new uninfected MT-2 cells. The cells harvested at the end of each passage were subjected to direct sequencing, and the viral population change was determined by the relative peak height in the sequencing chromatogram. The persistence of the original amino acid substitution was confirmed in all infectious clones used in this assay.

2.7. Molecular modeling studies

The programs SYBYL and O were used to prepare models of the complexes of wild-type, M184V, and insertion mutant HIV-1 RT with DNA and the triphosphates of 3TC and EFdA. The starting atomic coordinates of HIV-1 RT were from the structure described by Huang et al. (PDB code 1RTD) (Huang et al., 1998). The side-chain mutations were manually modeled using mostly conformations encountered in RT structures that carry such mutations. The local structures of mutants were optimized using energy minimization protocols in SYBYL. The triphosphates of the inhibitors were built based on the structures of dTTP in

Table 1
Antiviral activity against HIV-1 and HIV-2 strains in MT-4 cells

Compound (abbreviation)	EC_{50} (μM)[a]		Selectivity[b]	
	HIV-1_{IIIB}	HIV-2_{EHO}	CC_{50} (μM)[c]	index
2′-Deoxy-4′-C-ethynyl-adenosine (EdA)	0.0095 ± 0.0027[d]	0.006 ± 0.0015	104 ± 6.2	11,000
2′-Deoxy-4′-C-ethynyl-2-fluoroadenosine (EFdA)	0.000073 ± 0.000017	0.000098 ± 0.000022	9.8 ± 3.4	134,000
2′,3′-Dideoxy-4′-C-ethynyl-2-fluoroadenosine (EFddA)	1.17 ± 0.29	1.07 ± 0.23	230 ± 33	196
2′,3′-Didehydro-3′-deoxy-4′-C-ethynyl-2-fluoroadenosine (EFd4A)	0.11 ± 0.033	0.089 ± 0.0007	98 ± 26	899
2′-Deoxy-4′-C-cyano-2-fluoroadenosine (CNFdA)	0.1 ± 0.034	0.09 ± 0.0087	>340	>3,300
2′-Deoxy-4′-C-ethynyl-2-chloroadenosine (ECldA)	0.00069 ± 0.00018	0.0006 ± 0.0000028	230 ± 16	339,000
2′,3′-Dideoxyinosine (ddI)	27 ± 12	24 ± 4.4	>100	>4
3′-Azido-3′-deoxythymidine (AZT)	0.0028 ± 0.00062	0.0022 ± 0.00073	30 ± 7.2	10,800

Anti-HIV activity was determined by the MTT method.
[a] EC_{50} represents the concentration that blocks HIV-1 replication by 50%.
[b] Selectivity index is calculated by the CC_{50}/EC_{50} for HIV-1_{IIIB}.
[c] CC_{50} represents the concentration that suppress the viability of HIV-1-unexposed cells by 50%.
[d] Data shown are mean values with standard deviations for at least three independent experiments.

1RTD, or of tenofovir diphosphate in the ternary complex of HIV-1 RT/DNA/TFV-DP (Tuske et al., 2004).

3. Results

3.1. Antiviral activity of 4′- and 2-substituted deoxyadenosine analogs

We evaluated the activity of 4′- and 2-substituted deoxyadenosine analogs against HIV-1 with the MTT assay using MT-4 cells. The 2′-deoxy-4′-C-ethynyl nucleoside with adenine as the base (EdA) exerted comparable activity to AZT (Table 1). 2-Fluoro substituted EdA, EFdA, was the most potent against HIV-1 with a sub-nanomolar EC_{50} of 0.073 nM. Selectivity of EFdA and ECldA was much increased compared to parental EdA or AZT. However, EFdA was also relatively cytotoxic compared to other inhibitors of this series. The 2-chloro (Cl) substitution also provided enhanced activity but with a decreased toxicity. Further modifications of the sugar ring from 2′-deoxyribose to 2′,3′-dideoxy- or 2′,3′-didehydro-2′,3′-dideoxy-ribose (EFddA or EFd4A) resulted in a drastic decrease of inhibitory potential. Substitution of the 4′-E group with a structurally similar 4′-cyano group also resulted in markedly decreased inhibitory activity. These results indicate that the 3′-OH and 4′-E moieties in the sugar ring are indispensable for high efficacy, and that antiviral activities are augmented by the modification with F- or Cl-moiety at the adenine 2-position. These compounds suppressed the replication of HIV-2 at comparable levels as HIV-1, consistent with the hypothesis that they act as nucleoside reverse transcriptase inhibitors (De Clercq, 1998).

3.2. Antiviral activity against HIV-1 variants resistant to NRTIs

To assess the effect of 4′- and 2-substituted adenosine analogs against drug resistant HIV-1, we generated recombinant infectious clones carrying various NRTI resistant mutations and tested them using the MAGI assay. We found that EdA, EFdA, and ECldA efficiently suppressed many of the viruses resistant to approved NRTI including the multi-drug resistant (MDR) virus, although the 3TC-resistant variant HIV-1_{M184V} and the multi-drug resistant variant HIV-$1_{M41L/T69SSG/T215Y}$ (Winters et al., 1998) showed modestly increased EC_{50} values to these compounds (Table 2). Interestingly, highly active 4′-E analogs, which have 3′-OH such as EFdA or ECldA, were even more effective against the dideoxy-type NRTI resistant variants K65R, L74V, and Q151M complex than they were against WT RT (Table 2). In contrast, 4′-E analogs without 3′-OH (EFddA and EFd4A) were similar or less effective with these resistant variants compared to WT, although the effect seems to be minimal. EFd4A and 2′-deoxy-4′-C-cyano-2-fluoroadenosine (CNFdA) were moderately active against HIV-1_{WT} and HIV-1_{MDR} (Shirasaka et al., 1995), but less active against HIV-1_{M184V}. Susceptibility of even the least active EFddA was still in the low micromolar range, but decreased against both HIV-1_{M184V} and HIV-1_{MDR}, by 84- and 13-fold, respectively.

3.3. Antiviral activity of EFdA against multi-drug resistant clinical isolates

We went on to further characterize EFdA, the most potent compound of the series, against clinical isolates from patients exposed to many anti-AIDS drugs. Five multi-drug resistant strains (HIV-1_{IVR405}, HIV-1_{IVR406}, HIV-1_{IVR412}, HIV-1_{IVR413}, and HIV-1_{A03}), which contained various drug-resistance mutations in HIV-1 genes (Table 3), were used. These clinical isolates showed high resistance to AZT, 3TC (HIV-1_{IVR406}), and ddI (HIV-1_{IVR412}). HIV-1_{IVR415} was also a drug-experienced virus but did not have NRTI-resistance mutations and showed no resistance, or less resistance to the NRTIs tested. Hence, it was used as a drug-sensitive HIV-1. Although antiviral activity of EFdA was slightly reduced against HIV-$1_{IVR405, IVR406, IVR412}$ (5.7- to 7.6-fold) compared to HIV-1_{IVR415}, the activity was high enough to suppress viral replication. It should be emphasized that EFdA was active against HIV-1_{IVR406}, which had the 3TC-resistant M184I substitution.

To evaluate antiviral activity of EFdA to M184V containing isolates in detail, two isolates harboring M184V were used. We used the MAGI assay that directly determines inhibition on a single replication cycle of HIV-1, so that we could eliminate the possible effects of multiple repli-

Table 2
Anti HIV-1 activity against drug-resistant infectious clones

	EC_{50} (μM)[a]								
	EdA	EFdA	EFddA	EFd4A	CNFdA	ECldA	ddI	AZT	3TC
WT	0.021	0.0011	1.2	0.35	0.21	0.0064	4.1	0.015	0.71
K65R	0.0082	0.00023 (×0.2)	1.56	0.2	ND[b]	0.0017 (×0.3)	ND	0.0039 (×0.3)	ND
L74V	0.01	0.00048 (×0.4)	2.52	0.54	ND	0.0015 (×0.2)	14.6	0.019 (×1.3)	ND
V75T	0.0075	0.00067 (×0.6)	9.13	0.95	ND	0.005 (×0.8)	ND	0.047 (×3.1)	ND
M41L/T215Y	0.062	0.0016 (×1.5)	6.7	1.67	ND	0.0065 (×0.1)	ND	0.12 (×8)	ND
M41L/T69SSG/T215Y[c]	0.18	0.0065 (×6)	ND	ND	ND	0.025 (×4)	21	0.20 (×13)	9.9
MDR[d]	0.011	0.00074 (×0.7)	16	0.46	0.69	0.0057 (×0.9)	40	18 (×1200)	1.1
P119S	0.018	0.00067 (×0.6)	ND	ND	ND	0.0062 (×1)	ND	0.0033 (×0.2)	0.6
T165A	0.045	0.001 (×0.9)	ND	ND	ND	0.0082 (×1.3)	ND	ND	0.66
I142V	0.077	0.001 (×0.9)	ND	ND	ND	0.0062 (×1)	ND	0.016 (×1)	0.36
T165R	0.088	0.0016 (×1.5)	ND	ND	ND	0.012 (×1.9)	ND	0.011 (×0.7)	0.28
M184V	0.088	0.0083 (×7.5)	101	6.41	1.76	0.084 (×13)	ND	0.0021 (×0.1)	>100
T165R/M184V	0.6	0.014 (×13)	ND	ND	ND	0.17 (×27)	ND	0.0053 (×0.4)	>100
I142V/T165R/M184V	0.81	0.023 (×22)	ND	ND	ND	0.41 (×65)	ND	0.0076 (×0.5)	>100
T165A/M184V[e]	0.43	0.015 (×14)	ND	ND	ND	0.16 (×25)	ND	0.0049 (×0.3)	>100
P119S/T165A/M184V[e]	0.5	0.015 (×14)	ND	ND	ND	0.20 (×32)	ND	0.0043 (×0.3)	>100

Anti-HIV activity was determined with the MAGI assay.

[a] The data shown are mean values obtained from the results of at least three independent experiments.

[b] ND: not determined.

[c] HIV-1 variant contains T69S substitution and 6-base pair insertions between codons for 69 and 70 (Ser-Gly) with AZT resistant mutations M41L/T215Y (Winters et al., 1998).

[d] Multi-dideoxynucleoside resistant HIV-1 contains mutations (AGT-GGT, SG) in the *pol* region: A62V/V75I/F77L/F116Y/Q151M (Shirasaka et al., 1995).

[e] These variants were reported by Nitanda et al. during induction of Ed4T resistant variants.

cation cycles on measured antiviral activity. In this assay, EFdA effectively suppressed both replication of HIV-1_{IVR443} and HIV-1_{IVR463}. Compared to the EC_{50} value for HIV-1_{WT} in Table 2, reduction of the activity was less than 3-fold, suggesting that EFdA suppresses relatively efficiently 3TC-resistant variants with either M184I or M184V mutations.

3.4. ADA stability of EFdA

Cellular ADA is known to convert dA to dI through deamination. Phosphorylation of the deaminated dA analogs, e.g., dI, is less efficient, resulting in low conversion of the active triphosphate (TP) form. In order to assess if the activation of these compounds to their TP forms would be affected by the activity of ADA, we tested whether ADA can degrade EdA or EFdA. While EdA was almost completely deaminated after 90 min exposure to ADA, EFdA was not deaminated for up to at least 90 min (Fig. 2). These results indicate that the 2-halo-substitution in EdA confers significant resistance to degradation by ADA.

3.5. Phosphorylation of EFdA

Currently available NRTIs need to be converted to the TP form by host cellular kinases before incorporation into newly synthesized proviral DNA. It has been shown that the antiviral effect of NRTIs was reversed by the addition of their physiological counterpart 2′-deoxynucleosides (Bhalla et al., 1990; Mitsuya et al., 1985). To identify the phosphorylation pathway, we examined whether the antiviral activity of EFdA was reversed by the addition of 2′-deoxynucleosides. Surprisingly, the addition of dC decreased the antiviral activity of EFdA in a dose-dependent manner (Fig. 3). In contrast, dT and dG had no effect on the

Table 3
Antiviral activity of EFdA against clinical isolates

Clinical isolates	Amino acid substitutions in the reverse transcriptation	EC_{50} (μM)			
		AZT	ddI	3TC	EFdA
PBMCs[a]					
IVR405	M41L/E44D/D67G/V118I/Q151M/L210W/T215Y	1.76	2.45	0.55	0.0012
IVR406	M41L/E44D/D67N/V118I/M184I/L210W/T215Y/K219R	0.64	1.46	>10	0.0011
IVR412	M41L/E44D/V75L/A98S/L210W/T215F	3.97	9.11	0.83	0.0016
IVR413	M41L/E44D/D67N/V75L/A98S/V118I/L210W/T215Y/K219R	1.0	2.22	1.46	0.00021
A03	M41L/E44D/D67N/L74V/L100I/K103N/V118I/L210W/T215Y	0.53	2.15	0.49	0.0001
IVR415	None	0.0028	0.33	0.078	0.00021
MAGI cells[b]					
IVR443	I135T/Y181C/M184V	0.027	3.6	>100	0.0031
IVR463	M41L/E44D/D67N/M184V/H208Y/L210W/T215Y	0.31	7.5	>100	0.0032

All assays were performed in triplicate. AZT, ddI, and 3TC were served as a control.

[a] Antiviral activity was determined by the inhibition of p24 antigen production in the culture supernatant.

[b] HeLa-CD4/CCR5-LTR/β-gal cells was used for the MAGI assay.

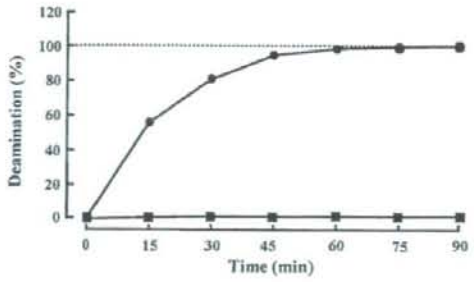

Fig. 2. Stability of EFdA following exposure to ADA. EdA or EFdA was incubated with ADA as described in Section 2. The deamination of adenine to inosine was analyzed by HPLC at indicated time points. The data represent the percent of starting compound (EdA; circle, EFdA; box) that was not deaminated by ADA.

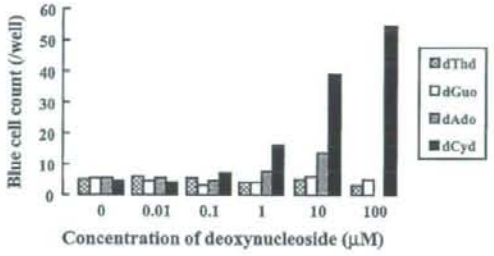

Fig. 3. Reversal of the antiviral activity of EFdA in the presence of 2′-deoxynucleosides. Each 2′-deoxynucleoside was added to the medium with serial dilution in the presence of EFdA (3.5 nM). The effect on EFdA activity was determined by the MAGI assay. An ADA inhibitor, dCF, was used during dA competition.

activity of EFdA. We could observe a slight reversal of the antiviral effect by addition of 10 μM dA with dCF. Effect of 100 μM dA could not be examined because of its cytotoxicity. It should be noted that all other tested analogs, including EFddA and EFd4A, were also reversed by the addition of dC (data not shown).

To confirm that the cellular dCK mediates the phosphorylation of EFdA, we examined the antiviral activity of EFdA in the HT-1080, dCK-deficient HT-1080/Ara-C^r (Obata et al., 2001), and dCK-transduced HT-1080/Ara-C^r cell lines. As expected, the antiviral activity of EFdA was markedly reduced in HT-1080/Ara-C^r cells (677-fold), but restored in dCK-transfected cells (Table 4). The same activity profile was observed with ddC, which is also phosphorylated by dCK (Starnes and Cheng, 1987). In contrast, AZT showed comparable activity among three cell lines, since it is known to be phophorylated mainly by thymidine kinase (Furman et al., 1986). Although dCK appears to be the main enzyme responsible for mono-phosphorylation of EFdA, other kinases, such as adenosine/deoxyadenosine kinases, may be partially involved in mono-phosphorylation of EFdA, especially since weak reduction in antiviral activity of EFdA was observed in addition of dA in high concentrations. Moreover, even in dCK-deficient HT-1080/Ara-C^r cells, EFdA exerted moderate antiviral activity. Hence, while it is possible that other kinases may be contributing to a smaller extent to the phosphorylation of EFdA, it appears that dCK is the enzyme that primarily phosphorylates this inhibitor.

3.6. Resistance to EFdA

In order to elucidate the mechanism of drug resistance to 4′-E analogs, we selected variants resistant to EdA, a parental compound of EFdA with the dose escalating methods (Nameki et al., 2005). After 58 passages in the presence of EdA, the resistant variants were obtained. Sequence analysis of the entire RT region revealed that a novel combination of mutations, I142V/T165R/M184V was introduced. Similar mutations (I119S/T165A/M184V) were observed in a Ed4T-resistant variant (Nitanda et al., 2005). Hence, we generated infectious clones containing these mutations and tested the antiviral activity of 4′-E analogs against them (Table 2). Mutation in T165, either Arg or Ala, enhanced the resistance against EdA, EFdA, and ECldA in the presence of the M184V mutation. Similar resistance profiles were observed for the I142V/M184V mutations. Furthermore, the triple mutant HIV-$1_{I142V/T165R/M184V}$ had the highest resistance among all tested variants. On the other hand, I142V or T165R alone did not affect the antiviral activity of EFdA or ECldA, although EdA or EFddA showed slightly decreased susceptibility. These results suggest that M184V appears to be the main mutation responsible for 4′-E analog resistance, and the addition of I142V and/or T165R augments the effect of M184V.

3.7. Replication of resistant HIV-1

For acquisition of high-level resistance to EFdA as well as EdA, three mutations, I142V, T165R, and M184V were required as described above. To examine the effect of the mutations on the viral replication kinetics we performed an assay that follows production of p24 gag antigen. All clones with M184V showed reduced replication kinetics (Fig. 4A), consistent with the reports that introduction of M184V markedly impairs replication kinetics (Wainberg et al., 1996; Yoshimura et al., 1999). Introduc-

Table 4
The effect of dCK expression on the EFdA antiviral activity[a]

Cell	EC_{50} (μM)[b]		
	AZT	ddC	EFdA
HT-1080	0.0032 ± 0.001	0.75 ± 0.22	0.00031 ± 0.0001
HT-1080/Ara-C^r	0.0027 ± 0.0005 (0.84)	84 ± 15 (112)	0.21 ± 0.03 (677)
HT-1080/Ara-C^r/dCK	0.0025 ± 0.00074 (0.78)	0.51 ± 0.16 (0.68)	0.000098 ± 0.000034 (0.32)

[a] SEAP activity in the culture supernatants were determined on day 2 after virus infection.
[b] The data shown are mean ± S.D. and fold increase in EC_{50} compared to HT-1080 is shown in parentheses.

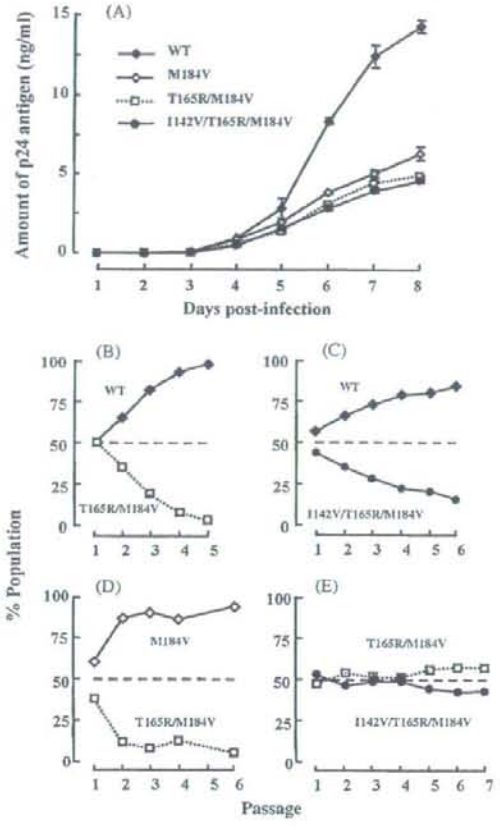

Fig. 4. Replication kinetics of HIV-1 clones with mutations. Production of p24 antigen in culture supernatant was determined with a commercially available p24 antigen kit. Profiles of replication kinetics (p24 production) of HIV-1_{WT} (closed diamonds), HIV-1_{M184V} (open diamonds), HIV-$1_{T165R/M184V}$ (open squares with broken line) and HIV-$1_{I142V/T165R/M184V}$ (open circles) were determined with MT-2 (A). Representative results from three independent triplicate determinations of p24 production with newly titrated viruses are shown. MT-2 cells were infected simultaneously with equal amounts of two HIV-1 clones to be compared. At each passage (5–6 days) the proviral sequences were determined and the percent population of each clone is reported at different passage; competition of WT and T165R/M184V (B); competition of WT with I142V/T165R/M184V (C); competition of M184V with T165R/M184V (D), and competition of T165R/M184V with I142V/T165R/M184V (E). At least two independent CHRAs were performed and are shown the representative results.

tion of T165R or I142V/T165R mutations in an M184V background (HIV-$1_{T165R/M184V}$ or HIV-$1_{I142V/T165R/M184V}$, respectively) further impaired HIV replication compared to HIV-1_{M184V}. I142V which enhanced EFdA resistance of HIV-$1_{T165R/M184V}$ (Table 2) conferred no replication rescue of HIV-$1_{T165R/M184V}$. To determine detailed replication kinetics, we performed CHRA which compares qualitatively viral replication. As shown in Fig. 4A, HIV-$1_{T165R/M184V}$ and HIV-$1_{I142V/T165R/M184V}$ showed reduced replication kinetics compared to HIV-1_{WT} (Fig. 4B and C). Replication kinetics ofHIV-$1_{I142V/T165R/M184V}$ was comparable to that of HIV-$1_{T165R/M184V}$, which showed further reduced replication kinetics compared to HIV-1_{M184V} (Fig. 4D and E). In another experiment, replication of HIV-$1_{I142V/T165R/M184V}$ was slightly decreased compared to HIV-$1_{T165R/M184V}$ (data not shown). These results suggest that introduction of three EdA mutations that also confers EFdA resistance impaired replication of HIV-1 in much greater extent compared to that of M184V.

4. Discussion

At present, HIV-1 variants containing NRTI-resistance mutations are widely observed not only in NRTI-experienced but also in NRTI-naïve patients. In such cases treatment failure is sometimes observed within short periods. The NRTI tenofovir, appears to be more effective against drug-experienced HIV-1 strains (Srinivas and Fridland, 1998). Unlike the other clinically available NRTIs, tenofovir has highly flexible acyclic ribose ring without a 3′-OH. Structural studies have suggested that the compact size of this inhibitor may contribute to the absence of highly resistant mutant strains against tenofovir (Tuske et al., 2004). Despite its unique structural profile, tenofovir is similar to other NRTIs in that it also lacks a 3′-OH group.

In contrast, the highly active 4′-E analogs such as EFdA retain the 3′-OH group of the canonical dNTP substrate. Similar to other NRTIs, they are also phosphorylated by cellular enzymes to their TP active form, which in turn serves as a substrate for HIV RT that incorporates them in an elongating primer during DNA synthesis. Following incorporation, replication is further inhibited by chain termination, although the specific mechanism of chain termination remains to be elucidated. Despite the fact that the 4′-E analogs have a 3′-OH like canonical dNTP substrates, cellular polymerases are likely to discriminate against these analogs, and not incorporate them during cellular DNA polymerization, as suggested by *in vitro* experiments with mitochondrial polymerase γ (Nakata et al., 2007). Alternatively, it is also possible that cellular proofreading systems excise the 4′-E analogs after their incorporation into cellular DNA.

The 3′-OH also plays an important role in phosphorylation of EdA analogs. Based on crystallographic results Sabini et al. reported that the interaction between 3′-OH of nucleosides and catalytic site of dCK was important for efficient nucleoside phosphorylation (Sabini et al., 2003). Alternatively, it is possible that the EFddA and EFd4A nucleosides that lack 3′-OH are poor substrates for HIV RT. The substitution at the 2-position of the purine base is also likely to contribute to highly potent *in vivo* activity of EF- or ECldA, possibly by preventing deamination of the inhibitor by ADA. ADA deaminates the adenine base into inosine, which is a poor substrate for cellular kinases. Similar ADA resistance has been reported for 2′-deoxy-2-chloroadenosine, a chemotherapeutic agent against hairy cell leukemia and chronic lymphocytic leukemia (Carson et al., 1980). ADA resistance may contribute to a longer intracellular half-life for EFdA-TP as compared to that of AZT (Nakata et al., 2007), indicating that substitution of 2-position plays an important role in sustained activity. When CEM cells were exposed to AZT or EFdA at concen-

tration of 0.1 μM, amounts of corresponding intracellular TP-forms were comparable (Nakata et al., 2007). However, inhibitory effect of EFdA in MT-4 and MAGI cells was approximately 40- and 15-fold superior compared to that of AZT (Tables 1 and 2). Taken together, HIV-1 RT appears to preferentially incorporate EFdA-TP compared to AZT-TP, although detailed enzymatic confirmation is needed. The parental EdA also seems to be a good substrate for HIV-1 RT; however, it may be subjected to deamination, resulting in comparable activity to AZT.

There are at least two mechanisms by which HIV RT can become resistant to NRTIs: first, HIV RT can acquire mutations at, or close to the dNTP-binding site, such that help it discriminate against NRTI-triphosphates, while it retains its ability to recognize the normal dNTP substrates (Huang et al., 1998). In the case of M184V/I the discrimination is based on steric conflict between a part of the inhibitor (the sulfur atom of the thioxolane ring in the case of 3TC), and the β-branched side chain of Val or Ile at the mutation site (Sarafianos et al., 1999). Mutations at other residues of the dNTP-binding site are responsible for discrimination of dideoxynucleosides from dNTPs during both the substrate-recognition (Martin et al., 1993) and the catalytic steps (Deval et al., 2002; Selmi et al., 2001). The other mechanism of NRTI resistance is based on an excision reaction (phosphorolysis) that unblocks NRTI-terminated primers using a molecule of ATP as the pyrophosphate donor (Meyer et al., 1999). The product of this reaction is a dinucleoside tetraphosphate and an unblocked primer that can continue viral DNA synthesis. In this case, the role of resistance mutations is to optimize binding of an ATP molecule that is used for the nucleophilic attack at the primer terminus. Most of AZT resistance as well as multi-NRTI resistance of RT with insertions at the fingers subdomain are thought to be based on an ATP-based unblocking mechanism. The insertions in RT destabilize the normally stable ternary complex (RT/template-primer/dNTP) and facilitate the ATP-mediated pyrophospholysis (Boyer et al., 2002). The fingers insertion mutant can excise all nucleotide analogs, with various degrees of efficiency.

Our molecular modeling studies are consistent with a mechanism of resistance to 4′-E analogs that involves steric hindrance between the 4′-E group of the inhibitors and the side chain of V184, reminiscent of the resistance mechanism to 3TC. While a single M184V mutation confers strong resistance to 3TC (>100-fold), it causes only moderate (8- to 13-fold) resistance to EFdA and ECIdA (Table 2). This is consistent with our molecular modeling analysis where the bulky and rigid 4′-E moiety appears to cause some steric hindrance with the Val or Ile side chain at position 184 during incorporation of the 4′-E nucleotides by the M184V enzyme (Fig. 5). The steric interaction appears to be stronger during incorporation of 3TC-TP (Fig. 5E) than EFdA-TP (Fig. 5C). Interestingly, the M184V mutation appears to confer stronger resistance to 4′-methyl substituted nucleotides, than to the 4′-ethynyl substituted nucleotides (Kodama et al., 2001). The decreased resistance of 4′-ethynyl substituted compounds may be in part the result of compensatory favorable interactions of the longer ethynyl group with residues of the dNTP binding site, including Y115 and D185. Such interactions may moderate the effect of the steric interactions of the 4′-ethynyl with residue V184 in the M184V mutant. Resistance of M184V to dideoxy-derivatives such as EFddA was unexpectedly high (84-fold). Although we cannot explain the detailed mechanism of the difference in resistance, it is possible that the presence of a 3′-OH in the EFdA (but not in the EFddA and EFd4A) results in more stabilizing interactions with residues such as Q151 that compensate for the steric hindrance by M184V (Fig. 5D). Hence, EFddA and EFd4A may be easier to push out of the binding pocket than analogs with a 3′-OH. For stronger resistance to 4′-E-2-halo-dAs, other mutations at positions 142 and 165 in addition to the M184V are required (Table 2) to substantially decrease inhibitor binding. It should be noted that the T165R/M184V mutations were also observed during induction of resistant variants to parental compound EdA. Nitanda et al. also reported that resistant variants for 4′-Ed4T contain M184V with T165A (Nitanda et al., 2005). As shown in Fig. 5A, the effect of the T165R mutation seems to be through the loss of a hydrogen bond between the side chain of Q182 and the side chain OH moiety of T165. Instead, there may be a hydrogen bond between C=O of the main chain of 184 and Q182 in the case of T165R/A, which would affect the positioning of the residue in position 184. Interestingly, HIV-2 has an Arg residue at position 165, whereas HIV-1 has Thr. We could not find decreased susceptibility in HIV-1_{T165R} or HIV-2, indicating that R165 becomes relevant only when Val is at the 184 position. When this residue is Met (T165R in M184 background), resistance is not affected substantially (1.5- to 2-fold resistance, Table 2) because of the flexibility of the Met side chain. However, when the 184 residue is Val (T165R/M184V), the position of 184 may be affected in a way that exacerbates the steric interactions between the ethynyl group of the incoming EFdA and the side chain of V184, resulting in resistance to EFdA and the other 4′-E analogs (13–27-fold resistance, Table 2). At this point it is not clear why the I142V mutation further augmented the effects of M184V and T165R. Finally, as shown in Fig. 5B, there are no apparent substantial steric problems for binding of EFdA to HIV-$1_{M41L/T69SSG/T215Y}$ RT, and the enzyme–inhibitor interactions are likely to be similar to those with dNTP and consistent with the relatively low resistance observed with this variant (Table 2) that is known to cause strong excision-based NRTI resistance. Crystallographic studies with the RT resistant variants complexed with the inhibitors should provide more insights into the mechanism of resistance.

The M184V, one of three mutations associated with EFdA resistance, develops rapidly under therapy with 3TC and has been reported to alter several profiles of RT function, including decreased RT processivity (Back et al., 1996), reduced nucleotide-dependent primer unblocking (Gotte et al., 2000), and increased fidelity (Wainberg et al., 1996). These profiles result in impaired viral fitness, hypersensitivity to other NRTIs, especially AZT (Larder et al., 1995), and delayed appearance of mutations, respectively. Our results show that modest resistance to EdA comes at a significant cost for the virus: The I142V and T165R mutations reduced even further viral replication kinetics of M184V-containing virus. Furthermore, the virus containing these mutations retains the AZT hyper-susceptibility which is induced by

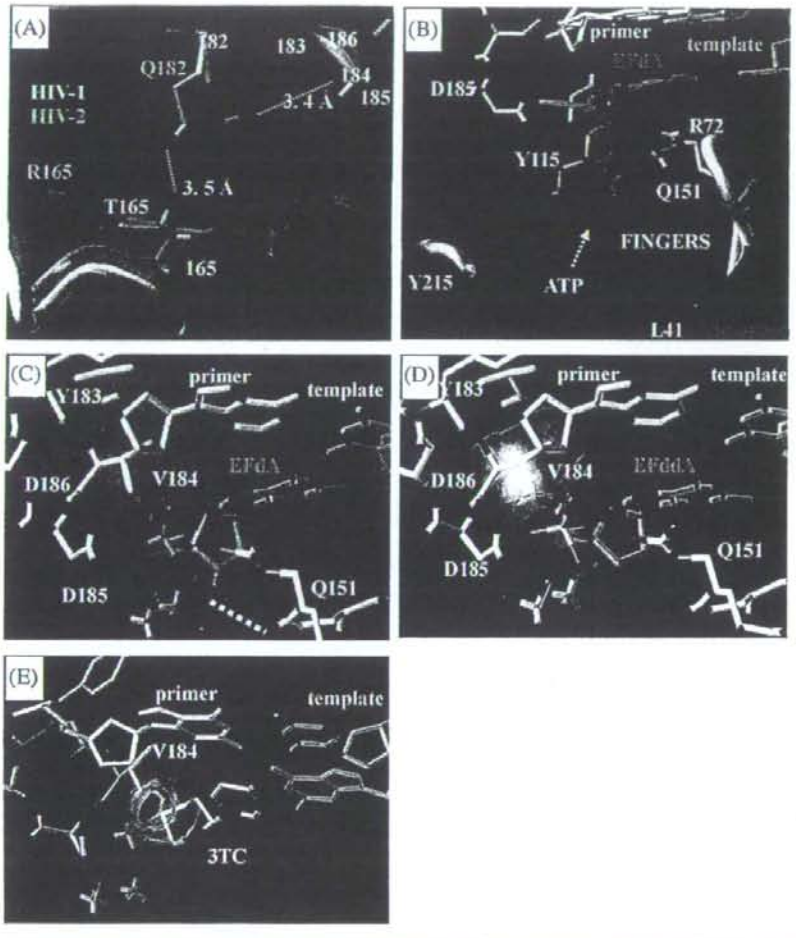

Fig. 5. Structural modeling of reverse transcriptase and compounds. (A) Superposition of the polymerase active sites of HIV-1 (gray) and HIV-2 (magenta) reverse transcriptases. Q182 makes a hydrogen bond with T165 in HIV-1. In the T165R mutant of HIV-1, the arginine side chain is expected to have a conformation similar to the one observed for R165 in HIV-2. In this context, Arg does not make a hydrogen bond with the side chain of residue 182 that may now interact with the main chain carbonyl of M184, which is at the immediate vicinity of the inhibitor-binding site. Such interaction may explain how the T165R mutation exacerbates the role of the M184V mutation in resistance to EFdA. (B) Proposed interactions of EFdA-triphosphate (TP) at the polymerase active site of the "fingers-insertion" NRTI-resistant HIV-1 RT, carrying the M41L/T69SSG/T215Y mutations. Possible steric interactions between the 4′-E group of EFdA-TP (C) or EFddA-TP (D) and the sulfur (S) of the pseudosugar ring of 3TC-TP (E). Van der Waals surfaces of 4′-E group (C and D) and S at sugar ring (E) are indicated in green and yellow. Possible steric interactions are shown as overalap of Van der Waal volumes of interacting atoms (in red).

M184V (Table 2), although further experiments are needed. These results suggest that the I142V and T165R mutations simply enhance resistance of M184V RT to EdA rather than optimize the viral fitness of the M184V virus. The increased cost for the virus to overcome inhibition pressure by EdA may have significant clinical benefits in the treatment of HIV infections.

Since EFdA is initially phosphorylated mainly by dCK and its activity was attenuated by addition of dC (data not shown), it is likely that dC analogs, such as 3TC and emtricitabine (FTC) that are mainly phosphorylated by dCK would act as a competitor of EFdA phosphorylation. However, one of dC analogs, apricitabine (ATC) showed little competition for the intracellular phosphorylation of 3TC and FTC (Bethell et al., 2007). Thus, interaction of NRTIs using identical phosphorylation enzymes should be carefully examined.

In conclusion, we have shown that the 2-halogen substituted EdAs have exceptionally potent subnanomolar antiviral activities. The 2-F substituted analog exhibited the highest potency and had a selectivity index significantly improved over that of approved NRTIs. In fact, results from our parallel studies with mice show no toxicity of EFdA (data not shown). The earlier studies also showed that a

parental nucleoside, EdA was not toxic in mice (Kohgo et al., 2004). The half-life of the intracellular TP form of EFdA is substantially extended (~17 h) compared to that of AZT (~3 h) (Nakata et al., 2007), suggesting that it may be possible to administer these inhibitors once a day. Further investigation may lead to their development as potential therapeutics against HIV infections.

Acknowledgements

We would like to thank S. Oka, T. Sasaki, M. Emerman, J. Overbaugh, K.-T. Jeang, M. Baba for providing HIV-1 clinical isolates, HT-1080 and HT-1080/Ara-C^r cell lines, HeLa-CD4-LTR/β-gal cells and HeLa-CD4/CCR5-LTR/β-gal cells through the AIDS Research and Reference Reagent Program, Division of AIDS, National Institute of Allergy and Infectious Diseases (Bethesda, MD), pNL101, pLTR-SEAP-puro, respectively. A.K. is supported by the 21st Century COE program of the ministry of Education, Culture, Sports, Science, and Technology. This work was supported by a grant for the promotion of AIDS Research from the Ministry of Health, Labor, and Welfare (E.K. and M.M.), a grant for Research for Health Sciences Focusing on Drug Innovation from The Japan Health Sciences Foundation (E.K. and M.M.).

References

Back NK, Nijhuis M, Keulen W, Boucher CA, Oude Essink BO, van Kuilenburg AB, et al. Reduced replication of 3TC-resistant HIV-1 variants in primary cells due to a processivity defect of the reverse transcriptase enzyme. EMBO J 1996;15(15):4040–9.

Bethell R, De Muys J, Lippens J, Richard A, Hamelin B, Ren C, et al. In vitro interactions between apricitabine and other deoxycytidine analogues. Antimicrob Agents Chemother 2007;51(8):2948–53.

Bhalla KN, Li GR, Grant S, Cole JT, MacLaughlin WW, Volsky DJ. The effect in vitro of 2′-deoxycytidine on the metabolism and cytotoxicity of 2′,3′-dideoxycytidine. AIDS 1990;4(5):427–31.

Boyer PL, Sarafianos SG, Arnold E, Hughes SH. Nucleoside analog resistance caused by insertions in the fingers of human immunodeficiency virus type 1 reverse transcriptase involves ATP-mediated excision. J Virol 2002;76(18):9143–51.

Carson DA, Wasson DB, Kaye J, Ullman B, Martin Jr DW, Robins RK, et al. Deoxycytidine kinase-mediated toxicity of deoxyadenosine analogs toward malignant human lymphoblasts in vitro and toward murine L1210 leukemia in vivo. Proc Natl Acad Sci USA 1980;77(11):6865–9.

De Clercq E. The role of non-nucleoside reverse transcriptase inhibitors (NNRTIs) in the therapy of HIV-1 infection. Antiviral Res 1998;38(3):153–79.

Deval J, Selmi B, Boretto J, Egloff MP, Guerreiro C, Sarfati S, et al. The molecular mechanism of multidrug resistance by the Q151M human immunodeficiency virus type 1 reverse transcriptase and its suppression using alpha-boranophosphate nucleotide analogues. J Biol Chem 2002;277(44):42097–104.

Dutschman GE, Grill SP, Gullen EA, Haraguchi K, Takeda S, Tanaka H, et al. Novel 4′-substituted stavudine analog with improved anti-human immunodeficiency virus activity and decreased cytotoxicity. Antimicrob Agents Chemother 2004;48(5):1640–6.

Furman PA, Fyfe JA, St Clair MH, Weinhold K, Rideout JL, Freeman GA, et al. Phosphorylation of 3′-azido-3′-deoxythymidine and selective interaction of the 5′-triphosphate with human immunodeficiency virus reverse transcriptase. Proc Natl Acad Sci USA 1986;83(21):8333–7.

Gotte M, Arion D, Parniak MA, Wainberg MA. The M184V mutation in the reverse transcriptase of human immunodeficiency virus type 1 impairs rescue of chain-terminated DNA synthesis. J Virol 2000;74(8):3579–85.

Haraguchi K, Takeda S, Tanaka H, Nitanda T, Baba M, Dutschman GE, et al. Synthesis of a highly active new anti-HIV agent 2′,3′-didehydro-3′-deoxy-4′-ethynylthymidine. Bioorg Med Chem Lett 2003;13(21):3775–7.

Huang H, Chopra R, Verdine GL, Harrison SC. Structure of a covalently trapped catalytic complex of HIV-1 reverse transcriptase: implications for drug resistance. Science 1998;282(5394):1669–75.

Jeang KT, Chun R, Lin NH, Gatignol A, Glabe CG, Fan H. In vitro and in vivo binding of human immunodeficiency virus type 1 Tat protein and Sp1 transcription factor. J Virol 1993;67(10):6224–33.

Kajiwara K, Kodama E, Matsuoka M. A novel colorimetric assay for CXCR4 and CCR5 tropic human immunodeficiency viruses. Antivir Chem Chemother 2006;17(4):215–23.

Kimpton J, Emerman M. Detection of replication-competent and pseudotyped human immunodeficiency virus with a sensitive cell line on the basis of activation of an integrated beta-galactosidase gene. J Virol 1992;66(4):2232–9.

Kodama EI, Kohgo S, Kitano K, Machida H, Gatanaga H, Shigeta S, et al. 4′-Ethynyl nucleoside analogs: potent inhibitors of multidrug-resistant human immunodeficiency virus variants in vitro. Antimicrob Agents Chemother 2001;45(5):1539–46.

Kohgo S, Yamada K, Kitano K, Iwai Y, Sakata S, Ashida N, et al. Design, efficient synthesis, and anti-HIV activity of 4′-C-cyano- and 4′-C-ethynyl-2′-deoxy purine nucleosides. Nucleosides Nucleotides Nucleic Acids 2004;23(4):671–90.

Kosalaraksa P, Kavlick MF, Maroun V, Le R, Mitsuya H. Comparative fitness of multi-dideoxynucleoside-resistant human immunodeficiency virus type 1 (HIV-1) in an In vitro competitive HIV-1 replication assay. J Virol 1999;73(7):5356–63.

Larder BA, Kemp SD, Harrigan PR. Potential mechanism for sustained antiretroviral efficacy of AZT-3TC combination therapy. Science 1995;269(5224):696–9.

Little SJ, Holte S, Routy JP, Daar ES, Markowitz M, Collier AC, et al. Antiretroviral-drug resistance among patients recently infected with HIV. N Engl J Med 2002;347(6):385–94.

Martin JL, Wilson JE, Haynes RL, Furman PA. Mechanism of resistance of human immunodeficiency virus type 1 to 2′,3′-dideoxyinosine. Proc Natl Acad Sci USA 1993;90(13):6135–9.

Meyer PR, Matsuura SE, Mian AM, So AG, Scott WA. A mechanism of AZT resistance: an increase in nucleotide-dependent primer unblocking by mutant HIV-1 reverse transcriptase. Mol Cell 1999;4(1):35–43.

Mitsuya H, Weinhold KJ, Furman PA, St Clair MH, Lehrman SN, Gallo RC, et al. 3′-Azido-3′-deoxythymidine (BW A509U): an antiviral agent that inhibits the infectivity and cytopathic effect of human T-lymphotropic virus type III/lymphadenopathy-associated virus in vitro. Proc Natl Acad Sci USA 1985;82(20):7096–100.

Miyake H, Iizawa Y, Baba M. Novel reporter T-cell line highly susceptible to both CCR5- and CXCR4-using human immunodeficiency virus type 1 and its application to drug susceptibility tests. J Clin Microbiol 2003;41(6):2515–21.

Nakata H, Amano M, Koh Y, Kodama E, Yang G, Bailey CM, et al. Activity against Human Immunodeficiency Virus Type 1, intracellular metabolism, and effects on human DNA polymerases of 4′-ethynyl-2-fluoro-2′-deoxyadenosine. Antimicrob Agents Chemother 2007;51(8):2701–8.

Nameki D, Kodama E, Ikeuchi M, Mabuchi N, Otaka A, Tamamura H, et al. Mutations conferring resistance to human immunodeficiency virus type 1 fusion inhibitors are restricted by gp41 and Rev-responsive element functions. J Virol 2005;79(2):764–70.

Nitanda T, Wang X, Kumamoto H, Haraguchi K, Tanaka H, Cheng YC, et al. Anti-human immunodeficiency virus type 1 activity and resistance profile of 2′,3′-didehydro-3′-deoxy-4′-ethynylthymidine in vitro. Antimicrob Agents Chemother 2005;49(8):3355–60.

Obata T, Endo Y, Tanaka M, Uchida H, Matsuda A, Sasaki T. Deletion mutants of human deoxycytidine kinase mRNA in cells resistant to antitumor cytosine nucleosides. Jpn J Cancer Res 2001;92(7):793–8.

Ohrui H. 2′-Deoxy-4′-C-ethynyl-2-fluoroadenosine, a nucleoside reverse transcriptase inhibitor, is highly potent against all human immunodeficiency viruses type 1 and has low toxicity. Chem Rec 2006;6(3):133–43.

Palella Jr FJ, Delaney KM, Moorman AC, Loveless MO, Fuhrer J, Satten GA, et al. Declining morbidity and mortality among patients with advanced human immunodeficiency virus infection. HIV Outpatient Study Investigators. N Engl J Med 1998;338(13):853–60.

Sabini E, Ort S, Monnerjahn C, Konrad M, Lavie A. Structure of human dCK suggests strategies to improve anticancer and antiviral therapy. Nat Struct Biol 2003;10(7):513–9.

Sarafianos SG, Das K, Clark Jr AD, Ding J, Boyer PL, Hughes SH, et al. Lamivudine (3TC) resistance in HIV-1 reverse transcriptase involves steric hindrance with beta-branched amino acids. Proc Natl Acad Sci USA 1999;96(18):10027–32.

Selmi B, Boretto J, Sarfati SR, Guerreiro C, Canard B. Mechanism-based suppression of dideoxynucleotide resistance by K65R human

immunodeficiency virus reverse transcriptase using an alpha-boranophosphate nucleoside analogue. J Biol Chem 2001;276(51):48466–72.

Shirasaka T, Kavlick MF, Ueno T, Gao WY, Kojima E, Alcaide ML, et al. Emergence of human immunodeficiency virus type 1 variants with resistance to multiple dideoxynucleosides in patients receiving therapy with dideoxynucleosides. Proc Natl Acad Sci USA 1995;92(6):2398–402.

Srinivas RV, Fridland A. Antiviral activities of 9-R-2-phosphonomethoxypropyl adenine (PMPA) and bis(isopropyloxymethylcarbonyl)PMPA against various drug-resistant human immunodeficiency virus strains. Antimicrob Agents Chemother 1998;42(6):1484–7.

Starnes MC, Cheng YC. Cellular metabolism of 2',3'-dideoxycytidine, a compound active against human immunodeficiency virus in vitro. J Biol Chem 1987;262(3):988–91.

Tuske S, Sarafianos SG, Clark Jr AD, Ding J, Naeger LK, White KL, et al. Structures of HIV-1 RT-DNA complexes before and after incorporation of the anti-AIDS drug tenofovir. Nat Struct Mol Biol 2004;11(5):469–74.

Wainberg MA, Drosopoulos WC, Salomon H, Hsu M, Borkow G, Parniak M, et al. Enhanced fidelity of 3TC-selected mutant HIV-1 reverse transcriptase. Science 1996;271(5253):1282–5.

Weiner MP, Costa GL, Schoettlin W, Cline J, Mathur E, Bauer JC. Site-directed mutagenesis of double-stranded DNA by the polymerase chain reaction. Gene 1994;151(1–2):119–23.

Winters MA, Coolley KL, Girard YA, Levee DJ, Hamdan H, Shafer RW, et al. A 6-basepair insert in the reverse transcriptase gene of human immunodeficiency virus type 1 confers resistance to multiple nucleoside inhibitors. J Clin Invest 1998;102(10):1769–75.

Yoshimura K, Feldman R, Kodama E, Kavlick MF, Qiu YL, Zemlicka J, et al. In vitro induction of human immunodeficiency virus type 1 variants resistant to phosphoralaninate prodrugs of Z-methylenecyclopropane nucleoside analogues. Antimicrob Agents Chemother 1999;43(10):2479–83.

ANTIMICROBIAL AGENTS AND CHEMOTHERAPY, June 2008, p. 2111–2119
0066-4804/08/$08.00+0 doi:10.1128/AAC.01299-07

Vol. 52, No. 6

Potent Synergistic Anti-Human Immunodeficiency Virus (HIV) Effects Using Combinations of the CCR5 Inhibitor Aplaviroc with Other Anti-HIV Drugs▽

Hirotomo Nakata,[1,2] Seth M. Steinberg,[3] Yasuhiro Koh,[2] Kenji Maeda,[1] Yoshikazu Takaoka,[4] Hirokazu Tamamura,[5] Nobutaka Fujii,[5] and Hiroaki Mitsuya[1,2]*

Experimental Retrovirology Section, HIV and AIDS Malignancy Branch, Center for Cancer Research, National Cancer Institute, National Institutes of Health, Bethesda, Maryland 20892[1]; Kumamoto University Graduate School of Medical and Pharmaceutical Sciences, Departments of Infectious Diseases and Hematology, Kumamoto 860-8556, Japan[2]; Biostatistics and Data Management Section, Center for Cancer Research, National Cancer Institute, National Institutes of Health, Bethesda, Maryland 20892[3]; Ono Pharmaceutical Co. Ltd., Osaka 618-8585, Japan[4]; and Graduate School of Pharmaceutical Sciences, Kyoto University, Sakyo-ku, Kyoto 606-8501, Japan[5]

Received 8 October 2007/Returned for modification 19 November 2007/Accepted 21 March 2008

Aplaviroc (AVC), an experimental CCR5 inhibitor, potently blocks in vitro the infection of R5-tropic human immunodeficiency virus type 1 (R5-HIV-1) at subnanomolar 50% inhibitory concentrations. Although maraviroc is presently clinically available, further studies are required to determine the role of CCR5 inhibitors in combinations with other drugs. Here we determined anti-HIV-1 activity using combinations of AVC with various anti-HIV-1 agents, including four U.S. Food and Drug Administration-approved drugs, two CCR5 inhibitors (TAK779 and SCH-C) and two CXCR4 inhibitors (AMD3100 and TE14011). Combination effects were defined as synergistic or antagonistic when the activity of drug A combined with B was statistically greater or less, respectively, than the additive effects of drugs A and A combined and drugs B and B combined by using the Combo method, described in this paper, which provides (i) a flexible choice of interaction models and (ii) the use of nonparametric statistical methods. Synergistic effects against R5-HIV-$1_{Ba\text{-}L}$ and a 50:50 mixture of R5-HIV-$1_{Ba\text{-}L}$ and X4-HIV-$1_{ERS104pre}$ (HIV-$1_{Ba\text{-}L/104pre}$) were seen when AVC was combined with zidovudine, nevirapine, indinavir, or enfuvirtide. Mild synergism and additivity were observed when AVC was combined with TAK779 and SCH-C, respectively. We also observed more potent synergism against HIV-$1_{Ba\text{-}L/104pre}$ when AVC was combined with AMD3100 or TE14011. The data demonstrate a tendency toward greater synergism with AVC plus either of the two CXCR4 inhibitors compared to the synergism obtained with combinations of AVC and other drugs, suggesting that the development of effective CXCR4 inhibitors may be important for increasing the efficacies of CCR5 inhibitors.

CCR5 is a member of the G-protein-coupled, seven-transmembrane-segment receptors, which comprise the largest superfamily of proteins in the body (30). In 1996, it was revealed that CCR5 serves as one of the two essential coreceptors for the entry of human immunodeficiency virus type 1 (HIV-1) into human $CD4^+$ cells, thereby serving as an attractive target for possible interventions against HIV-1 infection (1, 9, 40, 42). Consequently, scores of small-molecule CCR5 inhibitors which exert potent activity against R5-tropic HIV-1 (R5-HIV-1) were identified (2, 10, 19, 35). Aplaviroc (AVC), a spirodiketopiperazine derivative, represents one such experimental small-molecule CCR5 inhibitor (17, 18). AVC binds to human CCR5 with a high affinity, blocks HIV-1 gp120 binding to CCR5, and exerts potent activity against a wide spectrum of laboratory and primary R5-HIV-1 isolates, including multidrug-resistant HIV-1 isolates (50% inhibitory concentrations, 0.2 to 0.6 nM) (17, 18). Maraviroc (MVC) is another small-molecule CCR5 inhibitor which has become the first CCR5 inhibitor approved for the treatment of AIDS and HIV-1 infection by the U.S. Food and Drug Administration (FDA). One possible concern over the long-term use of CCR5 inhibitors is the change of viral tropism, which enables the virus to use the CXCR4 receptor (20, 41); therefore, CCR5 inhibitors are unlikely to be used as single agents. Assessments of the interaction of CCR5 inhibitors with other anti-HIV-1 agents should thus help provide an understanding of the role of CCR5 inhibitors and help design regimens to be used for the treatment of individuals infected with HIV-1.

In the present study, we determined the effects against R5-HIV-$1_{Ba\text{-}L}$ of AVC in combination with various anti-HIV-1 agents which affect other steps of the viral life cycle, including a nucleoside reverse transcriptase inhibitor, zidovudine (ZDV); a nonnucleoside reverse transcriptase inhibitor, nevirapine (NVP); a protease inhibitor, indinavir (IDV); and a fusion inhibitor, enfuvirtide (ENF). We assessed the synergistic effects of AVC in combination with CXCR4 inhibitors as well as the other drugs described above against a mixture of R5-HIV-$1_{Ba\text{-}L}$ and X4-HIV-$1_{ERS104pre}$ (designated HIV-$1_{Ba\text{-}L/104pre}$). In the present study, we also developed an evaluation system, designated the Combo method, which provides (i) a flexible choice of interaction models, (ii) the use of nonparametric statistical methods to obtain *P* values for comparison, and (iii) flexibility with respect to experimental design (e.g., checkerboard and constant-ratio designs). The present data suggest that AVC exerts antiviral synergy when it is

* Corresponding author. Mailing address: Departments of Infectious Diseases and Hematology, Kumamoto University School of Medicine, 1-1-1 Honjo, Kumamoto 860-8556, Japan. Phone: (81) 96-373-5156. Fax: (81) 96-363-5265. E-mail: hm21q@nih.gov.

▽ Published ahead of print on 31 March 2008.

used with other classes of anti-HIV-1 agents but apparently not when it is used with other CCR5 inhibitors. The present data also demonstrate a tendency toward greater synergism with AVC plus either of the two CXCR4 inhibitors examined in comparison to the synergism obtained with combinations of AVC and other FDA-approved drugs, suggesting that the development of effective CXCR4 inhibitors may be important for increasing the efficacies of CCR5 inhibitors.

MATERIALS AND METHODS

Antiviral agents. AVC is an experimental CCR5 inhibitor containing a spirodiketopiperazine core, as described previously (18, 19, 26). TAK779, SCH-C, and AMD3100 were synthesized as described previously (2, 7, 35). ZDV was purchased from Sigma (St. Louis, MO). IDV was kindly provided by Japan Energy Inc. (Tokyo, Japan). TE14011 and ENF were synthesized as described previously (36, 37). NVP was a kind gift from Boehringer Ingelheim Pharmaceuticals Inc. (Ridgefield, CT).

Viruses. R5-HIV-$1_{Ba\text{-}L}$ was obtained from the AIDS Research and Reference Reagent Program (13). X4-HIV-$1_{ERS104pre}$ was isolated from a drug-naïve patient with AIDS (33). These HIV-1 isolates were propagated in phytohemagglutinin-stimulated peripheral blood mononuclear cells (PHA-PBMCs), and the culture supernatants were harvested and stored at −80°C until use (22). In certain experiments, a 50:50 mixture of HIV-$1_{Ba\text{-}L}$ and HIV-$1_{ERS104pre}$ (HIV-$1_{Ba\text{-}L/104pre}$) was prepared.

Assay for in vitro anti-HIV-1 activity. PBMCs were isolated from the buffy coats of HIV-1-seronegative individuals by Ficoll-Hypaque density gradient centrifugation and were cultured at a concentration of 10^6 cells/ml in RPMI 1640-based culture medium supplemented with 10% fetal calf serum (FCS; HyClone Laboratories, Logan, UT), penicillin (50 U/ml), and streptomycin (50 μg/ml) (10% FCS–RPMI) with 10 μg/ml PHA for 3 days prior to the anti-HIV-1 activity assay in vitro. PHA-PBMCs (10^6/ml) from a 3-day culture were resuspended in 10% FCS–RPMI containing 10 ng/ml interleukin-2 and plated into each well of 96-well microculture plates (10^5 per well). Each of the test compounds was added as a single agent or in combination with another agent to each well of the microculture plates. For assessment of the effects of a combination of any two drugs, three threefold serial concentrations were chosen on the basis of the dose-response curve at which the percent inhibition values increased linearly.

The cells were subsequently exposed to 50 50% tissue culture infectious doses ($TCID_{50}$s) of HIV-$1_{Ba\text{-}L}$ or a mixture of 25 $TCID_{50}$s of HIV-$1_{Ba\text{-}L}$ and 25 $TCID_{50}$s of HIV-$1_{ERS104pre}$ and incubated at 37°C in humidified air containing 5% CO_2. On day 7 of culture, the cell-free culture supernatants were harvested and the HIV-1 p24 antigen levels in the supernatants were determined with a fully automated chemiluminescent enzyme immunoassay system (Lumipulse F; Fujirebio Inc., Tokyo, Japan) (18, 23). All the assays were performed in duplicate, and each experiment was conducted on 5 to 10 different occasions. No cytotoxicity was observed at the highest concentrations of each agent, as assessed by the trypan blue dye exclusion method.

Mathematical analysis: the Combo method. We assessed the effects of drug combinations using the combination index (CI), calculated with CalcuSyn software (BioSoft, Cambridge, United Kingdom), which was based on the median-effect method developed by Chou and Talalay (3, 4). For experiments with combinations of the same drug, serially diluted drug concentrations were chosen on the basis of the 50% effective concentrations (EC_{50}s), and each drug was combined with itself at the same concentration. As in the original method, CIs of <1, 1, and >1 were judged to represent synergism, additivity, and antagonism, respectively.

It should be noted that the Chou and Talalay median-effect method (3, 4) alone does not allow us to statistically compare the effects of the combinations. Thus, we devised a new method for evaluation of the effects of drug combinations, designated the Combo method. For the Combo method used in the present study, we used three concentrations of one drug (drug A) and three concentrations of the other drug (drug B) and combined the drugs at three different concentrations, preparing nine (3 × 3) combination cultures, and we obtained nine determinations of HIV-1 p24 concentrations (each combination assay was performed in duplicate). More precisely, three combinations were examined: the same drug A combination (drug A and drug A), the same drug B combination (drug B and drug B), and the combination of drug A and drug B. A full view of the data obtained with the drug combinations can be visualized (as shown in the Results section) in three-dimensional (3-D) figures by the use of Microsoft Excel software (version 11.0, 2004; Microsoft Corporation, Redmond, WA), based on the method of Prichard and colleagues (27, 28, 29). It is of note that with the Bliss independence method, the predicted additive effects at each combination point are subtracted from the inhibitory effects of the combination determined from the experimental drug combination assay, generating percent synergy values, and the points plotted above the predicted additive effects represent synergism, while the points below the plane represent antagonism. Using the Bliss independence method, we calculated percent synergy values for the nine determinations described above, and the average value was further computed, generating a mean percent synergy value (%$synergy^{mean}$). We repeated this assay for each drug combination 5 or 10 times on different occasions. These 5 or 10 %$synergy^{mean}$ values thus obtained for a set of combinations (drug A-drug A, drug B-drug B, and drug A-drug B) were compared with the other data sets (5 or 10 %$synergy^{mean}$ values) by the Wilcoxon rank sum test, generating P values for each combination set. All P values are two-tailed and have not been formally adjusted for multiple comparisons. However, in the context of the several experiments and comparisons performed, P values of <0.01 would clearly indicate statistical significance, while differences with values of $0.01 < P < 0.05$ would indicate strong trends.

TABLE 1. Anti-HIV-1 activity of each drug in the assay system

Virus	Compound	EC (nM) for anti-HIV-1 activity[a]			
		50%	75%	90%	95%
Ba-L	AVC	0.7 ± 0.4	4.0 ± 4.0	16 ± 15	25 ± 14
	SCH-C	6.8 ± 6.0	31 ± 18	94 ± 43	131 ± 64
	TAK779	20 ± 14	127 ± 83	332 ± 192	576 ± 224
	ZDV	18 ± 4.0	58 ± 3.0	128 ± 54	178 ± 49
	NVP	19 ± 2.0	36 ± 11	127 ± 39	149 ± 47
	IDV	29 ± 7.0	44 ± 12	75 ± 18	87 ± 13
	ENF	11 ± 4.0	46 ± 5.0	82 ± 14	98 ± 16
104pre	AMD3100	26 ± 8.0	96 ± 21	193 ± 51	257 ± 46
	TE14011	4.0 ± 1.0	16 ± 7.0	50 ± 11	78 ± 17

[a] The EC_{50}, EC_{75}, EC_{90}, and EC_{95} values were determined by using PHA-PBMCs isolated from three different donors and the inhibition of p24 Gag protein production as the end point. All assays were conducted in triplicate. The results shown represent the arithmetic means (±1 standard deviation) of the values from three independently conducted assays.

RESULTS

Activities of anti-HIV-1 agents in PHA-PBMCs. We first determined the antiviral potencies of seven anti-HIV-1 agents (AVC, SCH-C, TAK779, ZDV, NVP, IDV, and ENF) against HIV-$1_{Ba\text{-}L}$ employing PHA-PBMCs as target cells (Table 1). AVC had a potent inhibitory effect against HIV-$1_{Ba\text{-}L}$, with mean EC_{50}, EC_{75}, EC_{90}, and EC_{95} values of 0.7, 4, 16, and 25 nM, respectively. SCH-C and TAK779, which are both CCR5 inhibitors, also showed potent antiviral activity (but with less potent antiviral activity compared to that of AVC), with EC_{50}s of 6 and 20 nM, respectively. To determine the additive effects of AVC-AVC and AMD3100-AMD3100, we employed R5-HIV-$1_{Ba\text{-}L}$ and X4-HIV-$1_{ERS104pre}$ as the virus inocula, respectively, since AVC is inert against X4-HIV-1 and AMD3100 is inert against R5-HIV-1. These two agents were found to be potent against the virus, with EC_{50}s of 26 and 4 nM, respectively. No toxicity of any of the anti-HIV-1 agents was observed at concentrations up to 1.0 μM, as determined by examination of PHA-PBMCs (data not shown).

Same-drug combination and additivity. To determine whether combinations of two different anti-HIV-1 agents produced synergistic, additive, or antagonistic effects, we first attempted to establish an algorithm so that the effects of the combination of the same drug (i.e., drug A-drug A) represent

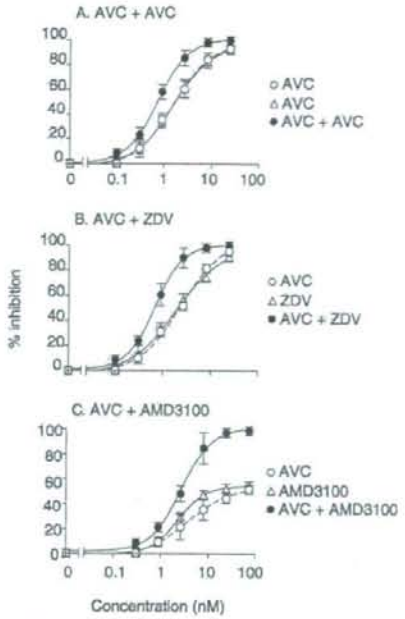

FIG. 1. Dose-response curves of single and combined drug assays. Three representative dose-response curves are shown. (A) Dose-response curve with the same-drug combination (AVC-AVC). PHA-PBMCs were exposed to R5-HIV-1_{Ba-L} and cultured in the presence of AVC alone or AVC-AVC over 7 days. AVC was serially diluted threefold to give concentrations in the range of 0.1 to 24.3 nM. The percent inhibition values were determined on the basis of the amounts of p24 Gag proteins in the culture supernatants. (B) AVC was combined with ZDV at a fixed ratio (1:11), and the assay was conducted as described above for panel A. (C) AVC (concentration range, 0.3 to 72.9 nM) was combined with AMD3100 at a 1:11 ratio. PHA-PBMCs were exposed to a 50:50 mixture of R5-HIV_{Ba-L} and X4-HIV-$1_{ERS104pre}$ and cultured in the presence of AVC alone, AMD3100 alone, or AVC-AMD3100. All assays were performed on 5 to 10 different occasions, and all the values shown represent the arithmetic means ± 1 standard deviation.

additivity. We determined the effects of combinations of the same drug for each of the seven anti-HIV-1 agents using the CIs dictated by the median-effect method (4). Figure 1A shows three representative dose-response curves of the percent inhibition of HIV-1 replication in the presence of a CCR5 inhibitor (AVC) alone, a reverse transcriptase inhibitor (ZDV) alone, a CXCR4 inhibitor (AMD3100) alone, or AVC plus AVC, ZDV, or AMD3100. A range of concentrations at which the percent inhibition values linearly increased was identified (Fig. 1A and B) and was used to examine the effects of any combination of two drugs chosen.

We found that the same-drug combination of AVC-AVC which gave a 50% reduction of HIV-1 replication produced a CI of 1.03 ± 0.09 (Table 2), indicating that this combination produced additivity on the basis of the median-effect method. However, that same-drug combination which gave 75, 90, and 95% reductions in viral replication produced CIs of 0.82, 0.71, and 0.68, respectively, which indicated that this same-drug combination produced synergistic effects. Synergistic effects were similarly indicated when the other anti-HIV-1 agents were examined as same-drug combinations in our analysis (Table 2).

The indication of synergism in the same-drug combination described above was thought to be a limitation or error inherent to the median-effect method or to stem from the variability of the biological data obtained. Since the median-effect method does not provide room for statistical analysis or a full view of the combination data, we examined the same data set using Microsoft Excel software, based on the method of Prichard and colleagues (27, 28, 29), which gives a graphical 3-D view of the entire data set. In the analysis of the AVC-AVC combination data, this method with Microsoft Excel software indicated that the combination of the highest AVC concentration (2.7 nM AVC and 2.7 nM AVC) that produced synergism gave a percent synergy value of 2.2, although other combinations were determined to be additive or antagonistic, giving an average (± standard deviation) percent synergy value of −1.8 ± 2.4 (Fig. 2A). The same-drug combinations of ZDV, NVP, and ENF similarly gave partial synergism (Fig. 2B, C, and E). However, the same-drug combination of IDV indicated synergism with all data points, with an average percent synergy value of 3.6 ± 2.2 (Fig. 2D). We predicted that the partial synergism seen with AVC, ZDV, NVP, and ENF and the entire synergism seen with IDV also represented a limitation or error inherent to the method of Prichard and colleagues (27, 28, 29) or the variability of the biological data obtained.

AVC acts in synergy with ZDV, NVP, IDV, and ENF to block the replication of HIV-1_{Ba-L} in PHA-PBMCs. Considering that one of the main reasons for the partial synergism described above could stem from the variability of the cell-based assay data used in the present work, we used standard nonparametric statistical analysis methods to evaluate the differences. To this end, we conducted the drug-combination assay in duplicate and determined the $\%synergy^{mean}$ values in three settings: (i) drug A-drug A, (ii) drug B-drug B, and (iii) drug A-drug B. Experiments testing the drug A-drug A combination and the drug B-drug B combination were conducted on 10 different occasions, while the drug A-drug B combinations assay was conducted on 5 different occasions. As shown in Fig. 3A, as

TABLE 2. CIs against HIV-1 obtained with mixtures of the same compounds at various inhibitory concentrations

Virus	Combination[b]	CI[a]			
		50%	75%	90%	95%
Ba-L	AVC + AVC	1.03 ± 0.09	0.82 ± 0.10	0.71 ± 0.10	0.68 ± 0.09
	ZDV + ZDV	1.08 ± 0.14	0.95 ± 0.18	0.84 ± 0.23	0.81 ± 0.22
	NVP + NVP	0.99 ± 0.09	0.81 ± 0.11	0.69 ± 0.12	0.66 ± 0.14
	IDV + IDV	1.02 ± 0.06	0.91 ± 0.05	0.79 ± 0.07	0.76 ± 0.06
	ENF + ENF	1.04 ± 0.08	0.89 ± 0.08	0.75 ± 0.09	0.73 ± 0.11
104pre	AMD + AMD	1.12 ± 0.12	0.88 ± 0.09	0.69 ± 0.09	0.67 ± 0.10
	TE + TE	1.05 ± 0.15	0.90 ± 0.11	0.80 ± 0.13	0.78 ± 0.13

[a] Drug interactions of same-drug combinations were analyzed by using CIs. CIs were calculated on the basis of the model of Chou and Talalay (3, 4) with CalcuSyn software (BioSoft). Originally, CIs of <1, 1, or >1 indicated a synergistic effect, an additive effect, and antagonism, respectively. The drugs were combined at a 1:1 ratio, and all assays were conducted in duplicate. The results shown represent the arithmetic means (±1 standard deviation) of the CIs at various inhibitory concentrations (50%, 75%, 90%, and 95%) from 10 independently conducted assays.

[b] AMD, AMD3100; TE, TE14011.

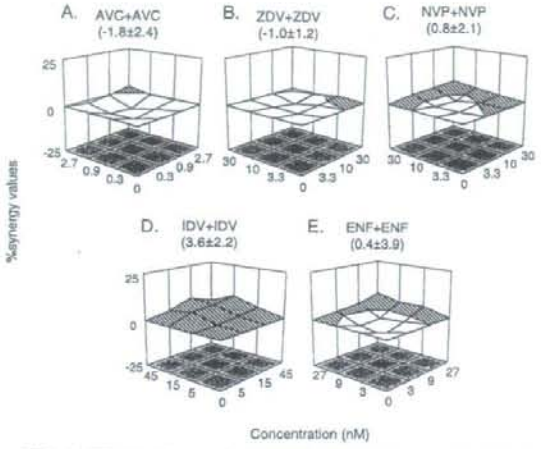

FIG. 2. Effects of same-drug combinations. The serially diluted anti-HIV-1 agents AVC (A), ZDV (B), NVP (C), IDV (D), and ENF (E) were combined with the same agent diluted under the same conditions; PHA-PBMCs were exposed to R5-HIV-1_{Ba-L} and cultured in the presence of the drugs combined. The combination effects (percent synergy values on the vertical z axis) were determined on the basis of the Bliss independence method. In the 3-D graphs, obtained on the basis of the method of Prichard et al. (27, 28, 29), the average percent synergy values at each concentration derived from 10 experiments were plotted. The hatched area represents synergism (percent synergy values, >0), while the open area represents additivity or antagonism (percent synergy values, ≤0). Numbers in parentheses represent the average percent synergy values (±1 standard deviation). The x and y axes indicate the concentrations of the drug tested (nM). All assays were performed in duplicate, and each experiment was independently conducted 10 times.

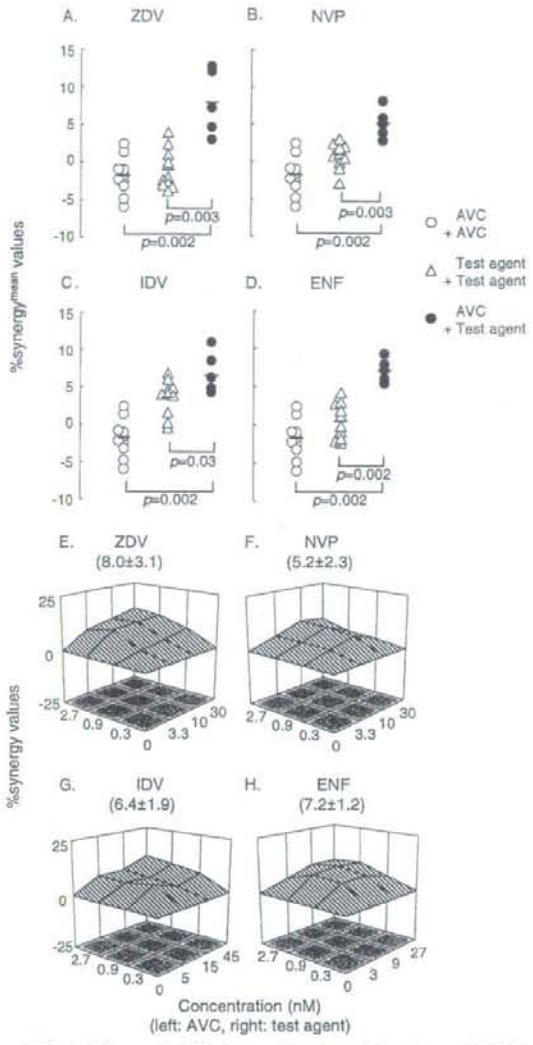

FIG. 3. Effects of AVC in combination with other anti-HIV-1 agents against R5-HIV-1_{Ba-L}. Drug combination assays were conducted, and the %synergy^{mean} values (the mean of the nine percent synergy values from each set of the data) are shown in three settings: (i) AVC-AVC, (ii) test agent (to be combined with AVC)-test agent, and (iii) AVC-test agent (A to D). The AVC-AVC combination and the test agent-test agent combination were tested on 10 different occasions, while the AVC-test agent combination assay was done on 5 different occasions. The differences in the %synergy^{mean} values between the three settings were analyzed by using the Wilcoxon rank sum test. The short bars indicate the arithmetic means. The combination effects are also shown in 3-D graphs, as determined on the basis of the method of Prichard et al. (see the legend to Fig. 2).

expected, the same-drug combination assays with AVC and ZDV produced relatively low average %synergy^{mean} values of −1.8 and −1.0, respectively. However, the AVC-ZDV combination gave a high average %synergy^{mean} value of 8.0. When we examined the difference among the AVC-AVC, ZDV-ZDV, and AVC-ZDV data using the Wilcoxon rank sum test, there was a statistically significant difference between the AVC-AVC and the AVC-ZDV data ($P = 0.002$) as well as between the ZDV-ZDV and the AVC-ZDV data ($P = 0.003$). The same was true when we examined the effects of NVP, IDV, and ENF in combination with AVC (Fig. 3B to D). With these data, we determined that if both the drug A-drug A and drug B-drug B combinations gave relatively low %synergy^{mean} values and a significant difference between the drug A-drug B combination and the same-drug combinations was detected, we would judge that there was significant synergism. When we plotted the average percent synergy value for the combination of drugs A and B at each different concentration on a point-by-point basis by the method of Prichard and colleagues (27, 28, 29), the results showed substantially higher levels of synergism for all data points (Fig. 3E to H). The average percent synergy values for AVC-ZDV, AVC-NVP, AVC-IDV, and AVC-ENF were 8.0 ± 3.1, 5.2 ± 2.3, 6.4 ± 1.9, and 7.2 ± 1.2, respectively, which corroborated the interpretation of the data shown in Fig. 3A to D. Thus, we interpreted that the addition of AVC to each of the other agents produced significant synergism.

Effects of AVC in combination with SCH-C or TAK779 against R5-HIV-1_{Ba-L}. We next asked whether AVC in combi-

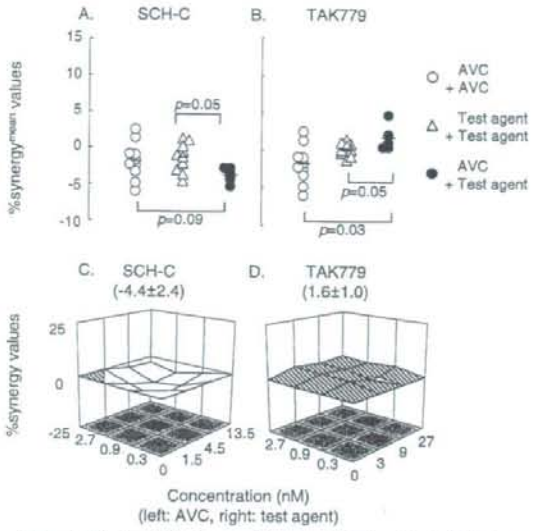

FIG. 4. Effects of AVC in combination with other CCR5 inhibitors. The effects of AVC in combination with SCH-C (A) or TAK779 (B) when they were exposed to R5-HIV-1_{Ba-L} are shown. No significant synergism was seen when AVC was combined with SCH-C or TAK779 compared with that seen with AVC-AVC. There was a trend toward antagonism when AVC–SCH-C with SCH-C–SCH-C and a trend toward synergism when AVC-TAK779 was compared with TAK779-TAK779. When these data were examined by the method of Prichard et al. (27, 29), AVC–SCH-C showed a mixed pattern but with an inclination toward antagonism (C), while AVC-TAK779 showed a mixed pattern but with an inclination toward synergy (D).

nation with SCH-C or TAK779 had synergistic activity against HIV-1_{Ba-L} (Fig. 4). The difference between the AVC-AVC and the AVC–SCH-C combinations was not statistically significant ($P = 0.09$), while there was evidence of a trend toward antagonism between the SCH-C–SCH-C and the AVC–SCH-C combinations ($P = 0.05$). It was interesting that when these data were examined by the method of Prichard and colleagues (27, 28, 29), a mixed pattern with an inclination toward antagonism was seen, with an average percent synergy of -4.4 ± 2.4. We also examined whether AVC had significant combination effects when it was combined with TAK779. There was a trend toward a statistically significant difference between AVC-AVC and AVC-TAK779 ($P = 0.03$) as well as TAK779-TAK779 and AVC-TAK779 ($P = 0.05$). However, when these data were plotted in the chart by the method of Prichard and colleagues (27, 28, 29), the pattern was a mixed one, with a low average percent synergy (1.6 ± 1.0), suggesting that synergism would be at a low level. However, it was noted that the same set of data for the combination of AVC and SCH-C produced CI values of 1.05 (at a 50% inhibitory effect) and 0.58 (at a 90% inhibitory effect), indicating that there was synergism between AVC and SCH-C, as analyzed on the basis of the median-effect method of Chou and Talalay (3, 4). It was thought that there was a propensity toward an overestimation of the combination effects toward synergism when the median-effect method was used.

Combination effects of AVC in a mixture of R5-HIV-1_{Ba-L} and X4-HIV-$1_{ERS104pre}$. AVC exerts no antiviral activity against X4-HIV-1 (18, 23), although the HIV-1 population seen in individuals with HIV-1 infection often comprises both R5- and X4-HIV-1 populations. Hence, it would be reasonable to use a CCR5 inhibitor plus a CXCR4 inhibitor to treat individuals with HIV-1 infection (6). Thus, we attempted to examine effects of the combination of AVC and either AMD3100 and TE14011 against HIV-$1_{Ba-L/104pre}$.

It is thought that the replication kinetics of HIV-1 strains tend to affect the results of any antiviral assay, in particular, when more than one HIV-1 isolate is employed in one assay. We therefore first conducted a set of experiments in order to delineate the replication curves for both the R5-tropic (HIV-1_{Ba-L}) and X4-tropic (HIV-$1_{ERS104pre}$) strains used in this study. It was confirmed that the two strains had comparable replication kinetics and that the p24 values of both strains were comparable over 7 days when the amount of each strain inoculated was adjusted on the basis of the $TCID_{50}$ for the strain (data not shown). Moreover, the amounts of HIV-1 p24 produced by PBMCs that were exposed to the mixture of the R5- and X4-tropic strains and cultured in the presence of a high concentration of AVC were comparable to the amounts of HIV-1 p24 from PBMCs that were similarly treated but that were cultured in the presence of a high concentration of AMD3100 (Fig. 1C). These data suggested that HIV-1_{Ba-L} and HIV-$1_{ERS104pre}$ replicate comparably in cell cultures inoculated with the 50:50 mixture of the viruses. To determine the additive effects of AVC-AVC and AMD3100-AMD3100, we employed R5-HIV-1_{Ba-L} and X4-HIV-$1_{ERS104pre}$ as the target viruses, respectively, since AVC is inert against X4-HIV-1 and AMD3100 is inert against R5-HIV-1.

The AVC-AMD3100 combinations produced %$synergy^{mean}$ values significantly different from those for AVC-AVC ($P = 0.002$) and those for AMD3100-AMD3100 ($P = 0.005$) (Fig. 5A). When these combination data were examined in the 3-D model of Prichard and colleagues (27, 28, 29), apparently high levels of synergism were seen for all data points, with an average percent synergy value of 8.0 ± 4.4 (Fig. 5G). When TE14011 was combined with AVC, synergism was similarly seen, with an average percent synergy value of 8.2 ± 4.5 (Fig. 5H). The %$synergy^{mean}$ values for AVC-ENF were also greater than those for AVC-AVC ($P = 0.005$) and less than those for ENF-ENF ($P = 0.04$); however, when the level of synergism was examined in the 3-D model, it appeared to be relatively lower, with an average percent synergy value of 4.8 ± 4.2 (Fig. 5I).

We next examined the effect of AVC in combination with one of the three FDA-approved anti-HIV-1 agents, ZDV, NVP, and IDV. The %$synergy^{mean}$ values obtained with AVC-ZDV or AVC-NVP were greater than those obtained with AVC-AVC, ZDV-ZDV, and NVP-NVP (P values for all comparisons, ≤ 0.005; Fig. 5D and E). In the 3-D model, synergism was also observed for ZDV and NVP in combination with AVC (Fig. 5J and K). AVC-IDV produced no significant difference in the %$synergy^{mean}$ values compared to those for IDV-IDV ($P = 0.2$), although the effect of AVC-IDV was significantly different from the effect of AVC-AVC (Fig. 5F), and a substantial level of percent synergy was also seen in the 3-D model (Fig. 5L).